



Synthesis of 1,4-dihydropyrazolo[4,3-*b*]indoles via intramolecular C(sp²)-N bond formation involving nitrene insertion, DFT study and their anticancer assessment

Manpreet Kaur^a, Vikrant Mehta^b, Aabid Abdullah Wani^c, Sahil Arora^a, Prasad V. Bharatam^c, Ashoke Sharon^d, Sandeep Singh^{b,*}, Raj Kumar^{a,*}

^a Laboratory for Drug Design and Synthesis, Department of Pharmaceutical Sciences and Natural Products, School of Pharmaceutical Sciences, Central University of Punjab, Bathinda-151401, Punjab, India

^b Department of Human Genetics and Molecular Medicine, Central University of Punjab, Bathinda-151401, Punjab, India

^c Department of Medicinal Chemistry, National Institute of Pharmaceutical Education and Research (NIPER), SAS, Nagar, India

^d Department of Chemistry, Birla Institute of Technology, Mesra, Ranchi, Jharkhand, 835215, India

ARTICLE INFO

Keywords:

1,4-Dihydropyrazolo[4,3-*b*]indoles
C–N bond formation
Cadogan Cyclization
DFT study
Cancer
Topoisomerase inhibitors

ABSTRACT

We herein report a new synthetic route for a series of unreported 1,4-dihydropyrazolo[4,3-*b*]indoles (**6–8**) via deoxygenation of *o*-nitrophenyl-substituted *N*-aryl pyrazoles and subsequent intramolecular (sp²)-N bond formation under microwave irradiation expedite modified Cadogan condition. This method allows access to NH-free as well as *N*-substituted fused indoles. DFT study and controlled experiments highlighted the role of nitrene insertion as one of the plausible reaction mechanisms. Furthermore, the target compounds exhibited cytotoxicity at low micromolar concentration against lung (A549), colon (HCT-116), and breast (MDA-MB-231, and MCF-7) cancer cell lines, induced the ROS generation and altered the mitochondrial membrane potential of highly aggressive MDA-MB-231 cells. Further investigations revealed that these compounds were selective Topo I (**6h**) or Topo II (**7a**, **7b**) inhibitors.

1. Introduction

C–N bond formation [1–3] offers opportunities to construct diverse *N*-heterocycles with broader applications in pharmaceuticals,[4] supramolecular chemistry,[5] crop protecting agents,[6] etc. The majority of the C–N bond formation methods such as Buchwald-Hartwig amination reaction,[7] Ugi reaction,[8] and Eschweiler-Clarke methylation reaction[9] either utilize amines, imines or amides as one of the starting materials (nitrogen source) in the presence or absence of metal and/or ligand to access heterocyclic skeletons. The admittance to molecular diversity has amplified inspiring enthusiasm among synthetic chemists from the past decade because of its vivacious role in drug discovery. It is, therefore, of high importance to introduce efficient methods to synthesize new compounds of pharmaceutical interests. Reactions involving intramolecular reductive cyclization of *o*-functionalized nitroarenes using a reductant to construct heterocycles[10–11] such as carbazoles,

[12] indazoles,[13] and indoles[14] are gaining significant importance as they involve the direct conversion of a nitro group into reactive nitrogen species. The Cadogan/Cadogan-Sundberg cyclization[15–16] is one of the well-studied reductive cyclization reactions for synthesizing these skeletons, and the literature is witnessed on their advancements. [1]

Cancer has been recognized as one of the major diseases which is causing mortality worldwide, thus remains a major health problem to resolve. From the last five years, almost 29% of the drugs have been approved by the US to treat various types of cancers.[17] Nowadays, to combat cancer, the anticancer treatment approach has been advanced to target-based drug discovery[18] like targeting topoisomerases (Topos), [19] epidermal growth factor receptor,[20] HDACs,[21] etc. as their overexpression mediate growth of a variety of cancers, especially lung, breast, ovary, colon, etc. Among these targets, topoisomerases, due to their role in maintaining the topology of DNA, are identified as one of

Abbreviations: CPT, Camptothecin; IC₅₀, Inhibitory Concentration at half-maximal; Topo, Topoisomerase; MTT, (3-(4,5-Dimethylthiazol-2-yl)-2,5-diphenyltetrazolium Bromide; ROS, Reactive Oxygen Species; MMP, Mitochondrial Membrane Potential.

* Corresponding authors.

E-mail addresses: sandeepsingh82@cup.edu.in, sandeepsingh82@gmail.com (S. Singh), raj.khunger@gmail.com, rajcps@cup.edu.in (R. Kumar).

<https://doi.org/10.1016/j.bioorg.2021.105114>

Received 27 April 2021; Received in revised form 17 June 2021; Accepted 18 June 2021

Available online 29 June 2021

0045-2068/© 2021 Elsevier Inc. All rights reserved.

the most important cellular targets for clinically potent anticancer agents.[22]

Indoles are attractive molecules due to their ubiquity in nature.[5,23–24] Heteroaryl-substituted or fused-indoles epitomize privileged architectural units frequently found in pharmaceuticals and bioactive molecules.[25] Sunitinib, indomethacin, pindolol, physostigmine, delavirdine, metralindole, vincristine, and sumatriptan are some of the FDA approved indole containing drugs for the treatment of cancer, cardiovascular and neurologic disorders (Fig. 1).[26]

Recently carbazoles, pyrazolocarbazoles and *N*-acetyl pyrazolines (Fig. 2) have emerged as potent anticancer agents via topoisomerase inhibition as one of their primary targets.[27–29] Considering the structural scaffolds of the compounds as mentioned above, we designed new 1,4-dihydropyrazolo[4,3-*b*]indoles as Topo I/II inhibitors based on merging of active pharmacophores and their preliminary docking (6 h; a representative compound) into the proteins, which rationalized their proposed inhibitory activity.

It was surprising to know that only a few synthetic methods to access pyrazolo[4,3-*b*] or [3,4-*b*]indole derivatives have been developed during the past decade (Scheme 1 a-c). These involve either intramolecular palladium-catalyzed Heck-type heteroarylation of *o*-bromoanilino-pyrazoles (Scheme 1a),[30] gold-catalyzed three-component annulation reaction of alkynes, hydrazines and ketone/aldehydes (Scheme 1b),[31] or a three-step one-pot process consisting of the iodination of indole-2-carbaldehyde under basic conditions, followed by hydrazone formation and intramolecular cross-coupling using copper iodide (Scheme 1c).[32] Besides, none of the methods offers an inexpensive methodology with diverse substitutions at N-1, C-3 and N-4 positions of 1,4-dihydropyrazolo[4,3-*b*]indoles.

We report herein the synthesis of unreported 1,4-dihydropyrazolo [4,3-*b*] indoles (6) and their derivatives (7 and 8) via intramolecular reductive cyclization of 5-(*o*-nitroaryl)-1,3-diaryl-1*H*-pyrazole (5) under modified-Cadogan conditions in the presence of a reductant (trivalent

phosphorus) and with or without an electrophile (BnCl) under microwave irradiations (Scheme 1d) along with DFT studies and their anti-cancer assessment.

2. Results and discussions

2.1. Chemistry

2.1.1. Optimisation of reaction conditions

To begin with, nitro-substituted precursors (5a-5j) were synthesized (Scheme S1; see supplementary material file) as per the methodology reported by our research group.[33] To determine the standard reaction conditions for the synthesis of target compounds, 5d was chosen as the model substrate. The standard Cadogan reaction conditions were selected that employ reductant, i.e. PPh₃ (3 equiv; method A) or P(OEt)₃ (3 equiv; method B) to carry out exhaustive deoxygenation of 5d (1 equiv) in different solvents at high temperature (Table 1).

The initial screening revealed that 6d was solely obtained (61%; entry 3, Table 1) under method A in carrying out the reaction of 5d in toluene at 180 °C for 20 min under MW, whereas method B yielded 6d (52%) along with 7d (18%) when 5d was heated under MW in toluene at 210 °C for 30 min (entry 12, Table 1). Reactions under solvent-free conditions failed to afford the desired products in method A or B (entries 1, 9 and 10, Table 1). Microwave heating of reaction[34] was found to accelerate the reaction rate and increase the yield in both the methods (compare entry 2 with 3; compare entry 11 with 12, Table 1) except under neat conditions. Further, non-polar solvent, particularly toluene, emerged as the best choice for both the methods amidst solvents such as 1,4-dioxane, DMF, CH₃CN, MeOH and water. Unexpectedly, *N*-ethoxy product (9d) was not obtained with method B, which is generally observed along with NH product in P(OEt)₃-mediated reductive cyclization.[1] Interestingly possible formation of compounds with dibenzo [*b,f*]pyrazolo[1,5-*d*][1,4]diazepine ring system (10d-12d, Table 1) was

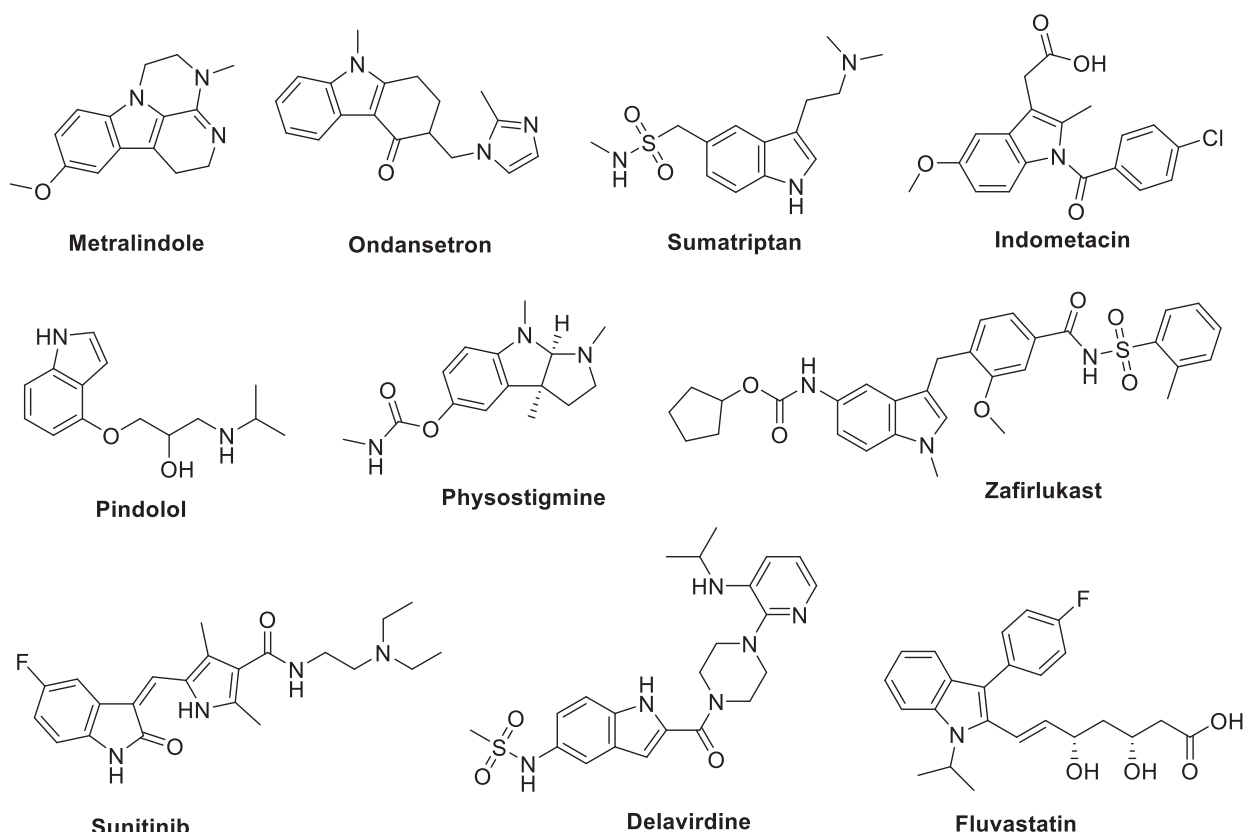


Fig. 1. Indole based FDA approved drugs.

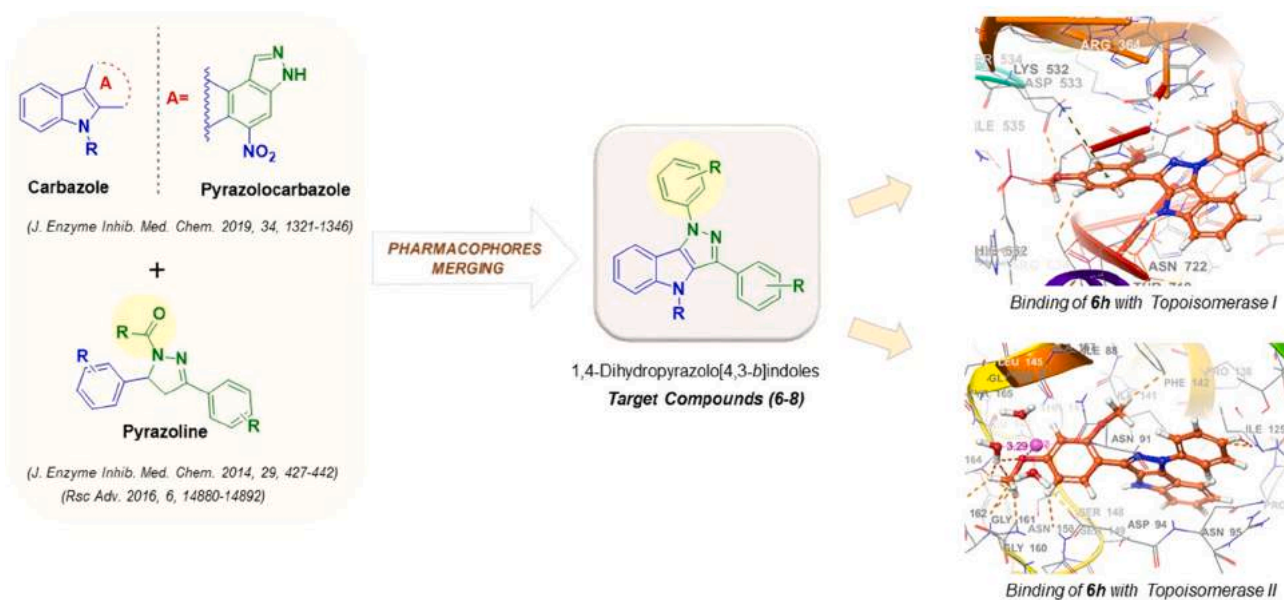


Fig. 2. Design of target compounds (6–8) as topoisomerase I/II inhibitors.

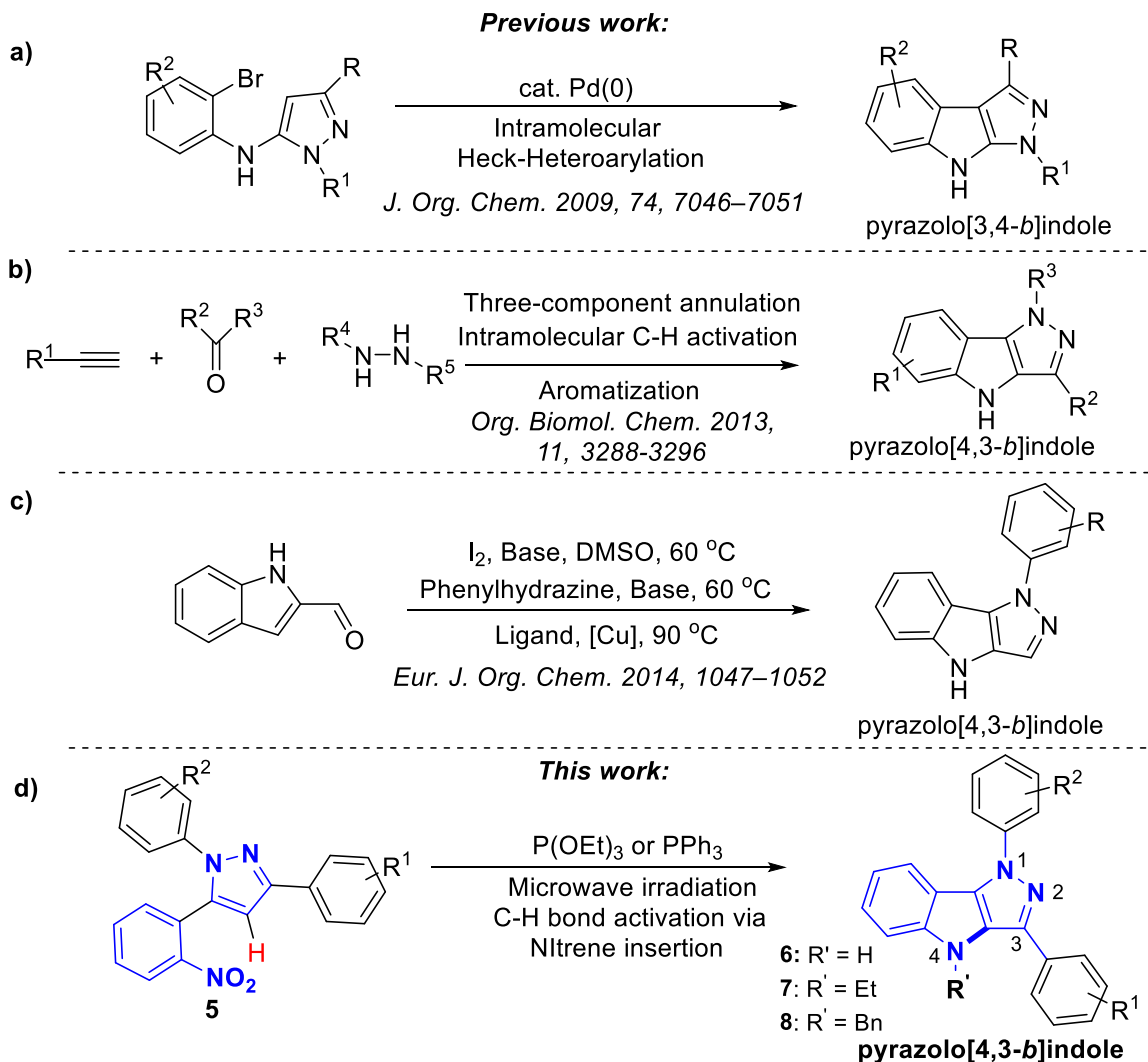
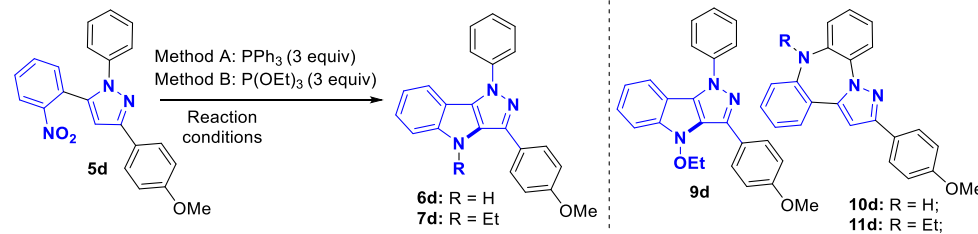
Scheme 1. Synthetic approaches for pyrazolo[4,3-*b*] or [3,4-*b*]indoles.

Table 1
Optimization of reaction conditions^a.



Entry	Solvent	Method	Reaction Conditions	6d	7d	Yield (%) ^b
1	–	A	180 °C, 24 h	Trace ^c	–	–
2	Toluene	A	Reflux, 24 h	22	–	–
3	Toluene	A	MW, 180 °C, 20 min	61 ^d	–	–
4	1,4-Dioxane	A	MW, 180 °C, 20 min	49	–	–
5	DMF	A	MW, 180 °C, 20 min	17	–	–
6	CH ₃ CN	A	MW, 180 °C, 20 min	15	–	–
7	MeOH	A	MW, 180 °C, 20 min	11	–	–
8	H ₂ O	A	MW, 180 °C, 20 min	–	–	–
9	–	B	Reflux, 24 h	3	Trace	–
10	–	B	MW, 210 °C, 30 min	8	3	–
11	Toluene	B	Reflux, 24 h	16	9	–
12	Toluene	B	MW, 210 °C, 30 min	52 ^d	18 ^d	–
13	1,4-Dioxane	B	MW, 210 °C, 30 min	29	10	–
14	DMF	B	MW, 210 °C, 30 min	19	9	–
15	CH ₃ CN	B	MW, 210 °C, 30 min	11	6	–
16	MeOH	B	MW, 210 °C, 30 min	7	2	–
17	H ₂ O	B	MW, 210 °C, 30 min	–	–	–

^a Substrate 5d (1 mmol, 1 equiv) was treated either with PPh₃ (3 equiv; method A) or P(OEt)₃ (3 equiv; method B), ^b Isolated yield, ^c reaction under MW (sealed tube) at 180 °C did not improve the yield. ^d Increase in time upto 2 h did not have much effect on the % yield.

also not detected.

To further explore the scope and limitations of reductive cyclization, nitro-substituted precursors were treated using method A or B under optimized conditions (Scheme 2a) to afford the target compounds (6 and 7). The reaction was found to be compatible with diverse functional groups on both the phenyl rings. For unknown reasons, corresponding products 6i and 6j of 5i and 5j were not obtained in method B.

Furthermore, the methodology was found to help construct *N*4 alkylated pyrazolo[4,3-*b*]indole *in situ*. For instance, when a mixture of 5d (1 equiv), PPh₃ (3 equiv) and benzyl chloride (1.5 equiv) was heated under MW irradiations (sealed tube) at 180 °C for 20 min, it resulted in the formation of *N*4-benzylated product (8d; 61%; Scheme 2b). This further extends the scope of methodology.

2.1.2. Mechanism of reaction (DFT study)

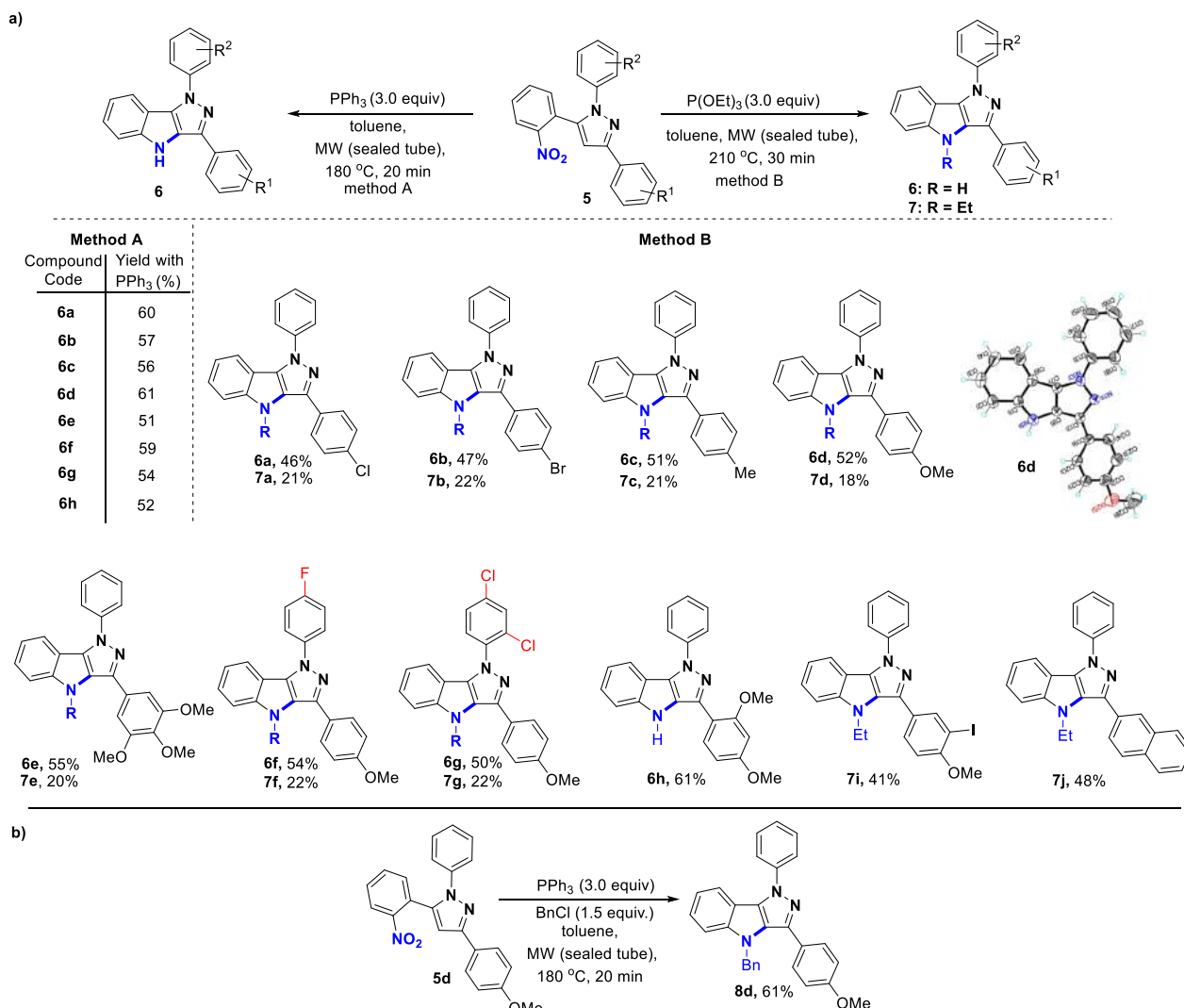
To understand the mechanism of reaction and formation of 6 and 7 under Cadogan conditions particularly using P(OEt)₃ as reductant, quantum chemical studies on 5k (R¹ = R² = R³ = R⁴ = R⁵ = R⁶ = H; a model substrate) were performed using Density Functional B3LYP and 6–31 + G(d) basis set (see Supplementary material). [35–37] The overall cyclization process was found to be thermodynamically favorable (Fig. 3) and exergonic by 70.59 kcal/mol, which can be seen from the free energy profile diagram (Fig. 4). The formation of products firstly involves the nucleophilic attack of the lone pair of P(OEt)₃ on the oxygen atom of the nitro of 5k followed by removal of PO(OEt)₃, resulting in the formation of nitroso intermediate 5ka. [16,38–42] Further, 5ka changes into product 6k via nitrene pathway, which involves deoxygenation of nitroso intermediate by P(OEt)₃ followed by the release of PO(OEt)₃ and formation of nitrene intermediate 5kb (Fig. 4).

The conformational analysis of 5kb revealed the possibility of another conformer, 5kb-C2. The formation of 5kb-C2 has been found to be endergonic by 4.18 kcal/mol (Fig. 4). The activation barrier required for the formation of the O–P bond in 5kb-C2 is 70.55 kcal/mol. The quantum chemical studies suggest the activation energy needed for the formation of the O–P bond in 5kb-C2 can serve as a rate-

limiting step for the formation of the product (6k). Two products are possible from 5kb-C2 along two different pathways (Pathway A and Pathway B; Fig. 3). Pathway A leads to the formation of *N*-OH (6kb) product, which is exergonic by 9.15 kcal/mol with an activation barrier of 30.39 kcal/mol, whereas Pathway B would lead to the formation of *N*-H (6k) product, which is exergonic by 78.85 kcal/mol with an activation barrier of 14.91 kcal/mol. The energetics of the two pathways and the experimental results motivated us to explore Pathway B (Fig. 3B), which involves the nitrene formation and its insertion to give the product. The formation of nitrene intermediate 5kc from 5kb-C2 is exergonic by 5.72 kcal/mol and hence is a thermodynamically favourable process.

The cyclization process involves the insertion of nitrene into the pyrazole C–H bond, resulting in the formation of a cyclized product which is exergonic by 69.05 kcal/mol. This insertion process involves an activation barrier of 14.91 kcal/mol. The role of triethyl phosphate of 5kb is to activate the pyrazole C–H bond, facilitating the nitrene insertion into the C–H bond of the pyrazole ring. Hence, triethyl phosphate here is analogous to iron which has been found to catalyze a similar kind of C–H activation followed by nitrene insertion and cyclization. [43].

Further, detection of a phosphorimidate byproduct in LC-MS (15d; Scheme S2) along with 6d, 7d and absence of *N*-OEt[44] product (9d) during a controlled experiment of 5d with in excess of P(OEt)₃ confirmed that present reaction occurs possibly via a nitrene mechanism and not by [13,16] non-nitrene pathway. The formation of *N*-substituted products like *N*-ethyl (ΔG = -1.71, E_a = 68.39) (7) and *N*-benzyl (ΔG = 6.08, E_a = 55.10) (8) can be justified as the products of nucleophilic substitution reactions of (6k) with the P(OEt)₃ and benzyl chloride, respectively under given reaction conditions. All the final products were new and fully characterized (mp, NMR, HRMS and X-ray; see SI).



Scheme 2. a and b. Synthesis of target compounds.

2.2. Biology

2.2.1. Evaluation of anticancer activity, alteration in mitochondrial membrane potential and redox parameter, and topoisomerase inhibition by the target compounds

All the target compounds were tested for cytotoxicity potential against A549 (lung), HCT-116 (colon), and MDA-MB-231 (breast), and MCF-7 (breast) cancer cell lines. All the compounds showed good antiproliferative activities (Table 2) with IC₅₀ values in the low micromolar range. The results were then represented from three independent experiments with the absorbance of the formazan formed in control (media only) cells taken as 100% viability, and the results of the MTT assay were plotted in graphical form (Fig. 5). Camptothecin (CPT) and etoposide were taken as reference drugs. Three different concentrations (1 μM, 5 μM, 25 μM) of the compounds were used, and treatments were given for 24 h. Although all the tested compounds exhibited low μM IC₅₀s, **7a**, **7b**, and **6h** emerged as broad-spectrum antiproliferative compounds (IC₅₀ range 0.58–2.41 μM; Table 2 and Fig. 5) comparable to standard drugs. Further, to determine the toxicity of these lead compounds on normal cells, we isolated human peripheral blood mononuclear cells (hPBMCs), and an MTT assay was performed. The results did not show any significant toxicity towards hPBMC tested at 10 and 25 μM concentration of the compounds for 48 h (Figure S2). After that, compounds were examined further for their various other impacts on cancer cells.

Compounds **6h**, **7a**, and **7b** were tested for Topo I mediated DNA relaxation assay to assess Topo I inhibitory potential. The results for Topo I inhibition assay showed that these chosen compounds exerted Topo I inhibitory activity. In the presence of Topo I inhibitor, the enzyme is unable to remove the supercoils. The inhibition of relaxation was measured by densitometry showing that compound **6h** showed better Topo I inhibition compared to camptothecin (Fig. 6A; Lane 7). **7a** (Lane 5) and **7b** (Lane 6) also displayed inhibition of Topo I mediated relaxation of supercoiled DNA though they were less effective than camptothecin (Fig. 6B).

Furthermore, for the Topo II inhibition assay, kDNA was used as a substrate for Topo II. Gel image shows that in the presence of Topo II, kDNA gets decatenated. However, in the presence of a Topo II inhibitor like etoposide, the decatenation gets reduced (Fig. 6 C; Lane 3). Interestingly, compounds **7a** and **7b** emerged as better Topo II inhibitors than etoposide. In contrast to these, compound **6h** (Lane 6) displayed weak Topo II inhibitory activity, and thus, we deduce that compound **7a** (Lane 4) and **7b** (Lane 5) are strong Topo II inhibitors (Fig. 6 D). Furthermore, topoisomerase binding assays revealed that **6h** inhibited Topo I, whereas **7a** and **7b** inhibited Topo II to a greater extent than the standard drugs.

This observation was further supported by *in silico* studies (Figure S3), which revealed some critical interactions (Fig. 6E and F), such as when **7a** docked at the Topo I binding site, it intercalates with

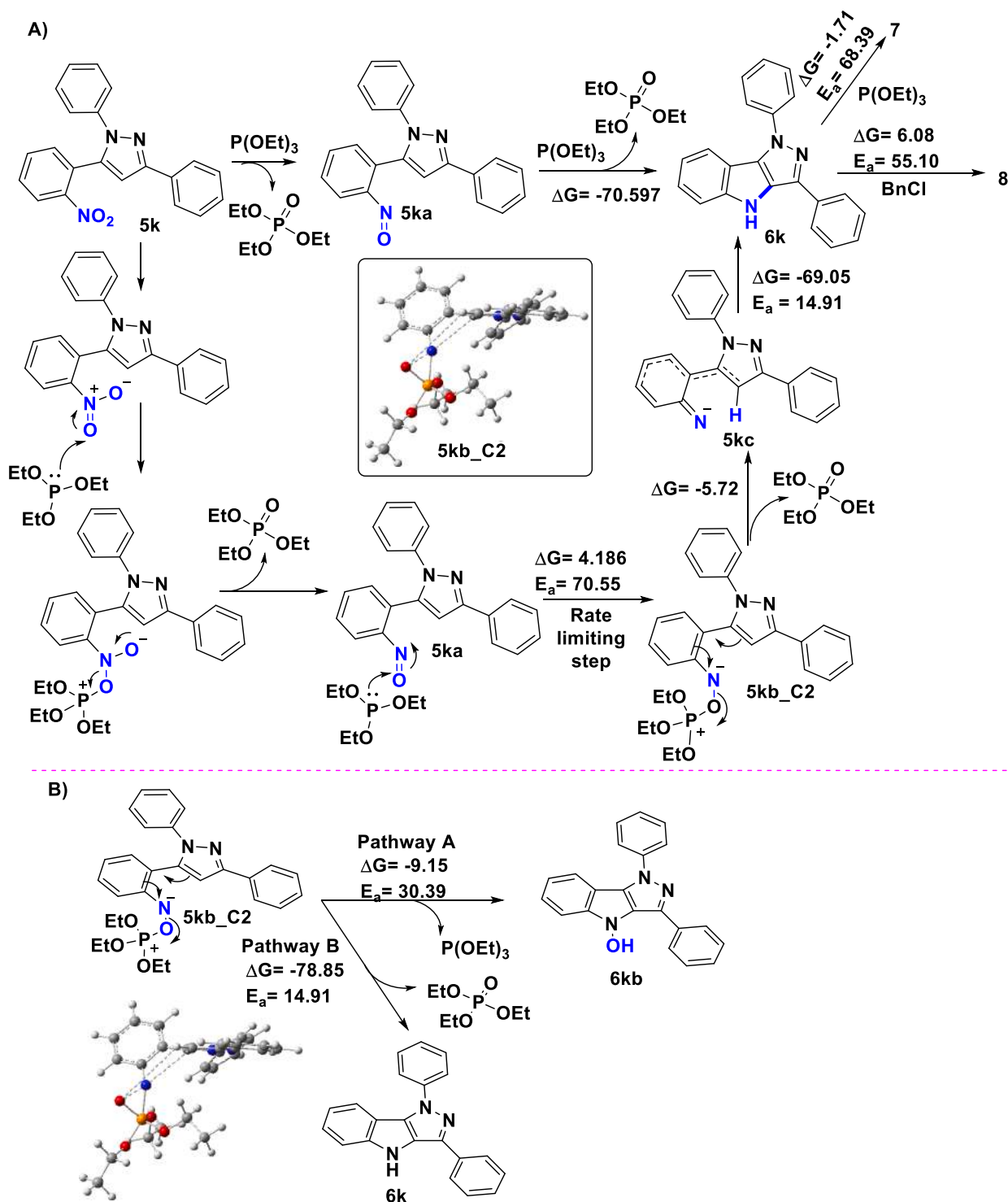


Fig. 3. A plausible mechanism of the reaction.

DNA and interacts with DG-12, DC-111, DC-112 residues. In addition, pyrazole ring nitrogen of **7a** showed hydrogen bonding with ARG364, and the aromatic hydrogens of two phenyl rings showed weak hydrogen bonding with ASP533. Furthermore, the docking of **7a** into Topo II disclosed that chlorine substituted phenyl ring displayed π -cation interactions with ARG98, weak hydrogen bonding with SER149. Interestingly, the 1,4-dihydropyrazolo[4,3-*b*]indole nucleus interacted with conserved Walker A motif lined by ARG162, ASN163, GLY164, TYR165, GLY166 and ALA167, responsible for Topo II inhibition.

Further, the tested compounds were investigated for their ability to

alter mitochondrial membrane potential (MMP) and ROS level in MDA-MB-231 cells. Interestingly, the studies revealed that these compounds modulated the MMP as indicated by an increase in the Red Green ratio leading to hyperpolarization of the membrane, as shown in Fig. 7.

Additionally, the intracellular ROS was measured by treating the washed cells with H2DCFDA (2', 7'-dichlorofluorescein diacetate) for 30 min at 37°C and then analyzed using a flow cytometer. This investigation revealed that compounds **7a**, **7b**, and **6h** induced oxidative stress, as evidenced by an upsurge in ROS generation compared to the control (Fig. 8).

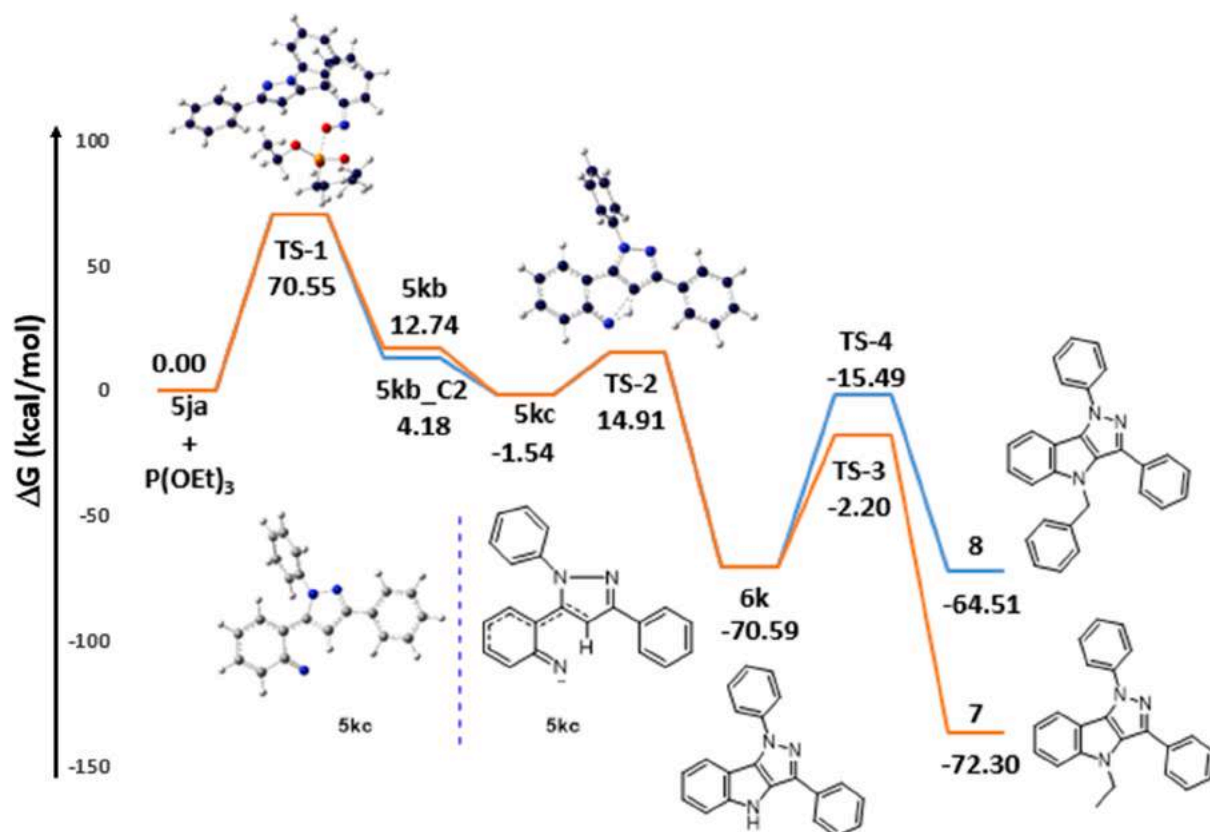


Fig. 4. Potential Energy Surface Diagram representing the cyclization process via nitrene pathway.

Therefore, from the biological evaluation, the investigation provided significant findings in the context of the anti-cancer potential of the synthesized compounds. Interestingly, all the compounds exhibited antiproliferative activity at a low micro-molar range, among which **6h**, **7a** and **7b** were the most effective compounds. The further elucidation of the anticancer mechanism revealed that **6h** inhibited topoisomerase I while **7a** and **7b** were potent topoisomerase II inhibitors. It is found from the literature that the cancer cells usually have fine-tuned ROS homeostasis, which allows them to operate pro-tumorigenic signaling without undergoing ROS induced cell death [45], and the cancer treatments like chemotherapy rely on generating ROS levels which activate intrinsic apoptosis [46]. Thus, to know about the mechanism of cell death, the compounds were further investigated, and it was found that our compounds were also able to induce cell death via ROS burst and hyperpolarisation of the mitochondrial membrane.

3. Conclusions

To encapsulate, we have described a new synthetic protocol for the construction of undocumented 1,4-dihydropyrazolo[4,3-*b*]indoles involving intramolecular C(sp²)-N bond formation under modified Cadogan reaction. DFT calculations rationalized the formation of products via the nitrene mechanism. The biological studies revealed that **7a**, **7b**, and **6h** were cytotoxic towards cancer cells, induced ROS generation and altered the mitochondrial membrane potential of highly aggressive MDA-MB-231 cells. Further investigations revealed that these compounds were selective Topo I (**6h**) or Topo II (**7a**, **7b**) inhibitors. Thus, the work offers the opportunity to synthesize products with substitution at N-1, C-3 and N-4 positions of 1,4-dihydropyrazolo[4,3-*b*]indoles required for further structure-activity relationship (SAR) study for pharmaceuticals as well as supramolecular chemistry perspective.

4. Experimental section

4.1. Chemistry

General Methods and Materials. Biotage® Initiator microwave synthesizer (Company: Biotage® Model No. 355,301 (Initiator EXPEU)) (used for sealed reactions) and Discover System; Company: CEM; Model No. 908010; Serial No. DU9671) (used for open reflux reactions) were used for carrying out microwave reactions at 200 W power. ¹H NMR and ¹³C NMR spectra were obtained in CDCl₃/d₆-DMSO on 400/500 MHz and 100/125 MHz Bruker Advance II NMR spectrometer/Jeol, respectively TMS (δ = 0) as an internal standard. Data were reported as follows: Chemical shifts (δ) are reported in ppm, coupling constants (*J*) are in Hertz (Hz). Abbreviations used to explain the multiplicities: s = singlet, d = doublet, t = triplet, q = quartet, m = multiplet. Column chromatography was performed with silica gel (60–120 and 100–200 mesh ASTM) to purify compounds. Melting points were measured with a melting point instrument and were uncorrected.

All the reagents were purchased from commercial suppliers and used without further purification. Reactions were monitored by TLC (detection with UV light).

General procedure for the synthesis of nitro precursors. (a) To a methanol solution containing acetophenones **1** (1.0 equiv) and 2-nitrobenzaldehyde **2** (1 equiv) was added NaOH (10%). The reaction mixture was stirred at room temperature for 2–3 h. After the completion of the reaction (TLC), the reaction mixture was poured into the water and filtered. The solid compounds (**3**) were washed with methanol and dried.

Analytical data of reference compound, 3a (precursor of 4a). (E)-1-(4-chlorophenyl)-3-(2-nitrophenyl)prop-2-en-1-one (**3a**). Cream yellow solid; 75% yield; ¹H NMR (500 MHz, DMSO-*d*₆): δ 8.22 (d, *J* = 7.8 Hz, 1H), 8.13–8.12 (m, 3H), 8.04–8.00 (m, 1H), 7.92–7.82 (m, 4H), 7.75–7.72 (m, 1H); ¹³C NMR (125 MHz, DMSO-*d*₆) δ 188.75,

Table 2

IC₅₀ values of synthesized compounds against various cancer cell lines.

Antiproliferative potential IC ₅₀ (μM) ^a	MDA-MB-231 (Breast)	MCF7 (Breast)	A549 (Lung)	HCT116 (Colon)
Compound Code				
6a	2.55 ± 0.21	2.6 ± 0.12	3.35 ± 0.32	2.8 ± 0.26
6b	3.22 ± 0.11	2.97 ± 0.32	2.84 ± 0.47	1.84 ± 0.1
6c	3.41 ± 0.51	2.65 ± 0.24	2.3 ± 0.29	2.7 ± 0.36
6d	2.3 ± 0.23	3.39 ± 0.18	2.78 ± 0.42	3.01 ± 0.3
6e	2.84 ± 0.27	2.6 ± 0.13	3.56 ± 0.3	2.87 ± 0.36
6f	2.34 ± 0.74	3.1 ± 0.69	4.72 ± 0.37	6.47 ± 0.11
6g	3.53 ± 0.42	2.89 ± 0.31	4.67 ± 0.59	4.14 ± 0.4
6h	1.58 ± 0.56	1.69 ± 0.26	1.87 ± 0.47	1.69 ± 0.2
7a	0.99 ± 0.24	1.29 ± 0.28	1.21 ± 0.50	1.47 ± 0.42
7b	0.84 ± 0.19	0.58 ± 0.13	1.63 ± 0.24	2.41 ± 0.44
7c	2.38 ± 0.21	3.28 ± 0.47	3.43 ± 0.51	2.99 ± 0.11
7d	2.49 ± 0.25	3.35 ± 0.41	3.24 ± 0.31	3.01 ± 0.27
7e	1.51 ± 0.29	2.53 ± 0.38	2.24 ± 0.45	3.01 ± 0.21
7f	2.34 ± 0.15	2.78 ± 0.36	3.24 ± 0.29	2.97 ± 0.39
7g	3.01 ± 0.14	2.84 ± 0.47	2.24 ± 0.16	3.03 ± 0.19
7i	2.43 ± 0.41	3.1 ± 0.24	3.28 ± 0.21	2.62 ± 0.17
7j	3.1 ± 0.1	3.25 ± 0.46	7.46 ± 0.16	3.76 ± 0.26
8d	3.22 ± 0.62	2.49 ± 0.23	3.41 ± 0.21	3.1 ± 0.32
Etoposide	2.05 ± 0.33	3.47 ± 0.41	3.14 ± 0.29	3.58 ± 0.28
Camptothecin (CPT)	0.21 ± 0.11	0.97 ± 0.27	1.65 ± 0.37	0.95 ± 0.3

^a Data was represented as mean ± S.E. from three independent experiments.; Camptothecin and Etoposide were taken as positive controls.

149.30, 139.51, 136.54, 134.27, 132.45, 131.68, 131.23, 130.14, 130.04, 128.24, 126.56, 125.23; MS (ESI): m/z = 287.7

(b) Further, **3** (1 mmol) were mixed with various substituted phenyl hydrazines (2–3 mmol) in methanol and refluxed for 3 h. The reaction was monitored by TLC, and the solvent was evaporated under vacuum to get **4**.

Analytical data of reference compound, 4a (precursor of 5a). 3-(4-chlorophenyl)-5-(2-nitrophenyl)-1-phenyl-4,5-dihydro-1H-pyrazole (**4a**). Peach solid; 93% yield; ¹H NMR (500 MHz, DMSO-*d*₆): δ 8.16 (d, *J* = 8.1 Hz, 1H), 7.77 (d, *J* = 8.5 Hz, 2H), 7.66 (t, *J* = 7.6 Hz, 1H), 7.56 (t, *J* = 7.7 Hz, 1H), 7.50 (m, 2H), 7.26 (t, *J* = 11.2 Hz, 1H), 7.18 (t, *J* = 7.9 Hz, 2H), 6.96 (d, *J* = 8.1 Hz, 2H), 6.76 (t, *J* = 7.3 Hz, 1H), 5.95–5.91 (m, 1H), 4.08 (m, 1H), 3.32–3.29 (m, 1H); ¹³C NMR (125 MHz, DMSO-*d*₆): δ 147.85, 147.12, 143.87, 136.72, 134.94, 133.79, 131.42, 129.57, 129.53, 129.18, 128.08, 127.96, 125.93, 119.60, 113.21, 60.53, 42.82; MS (ESI): m/z = 377.8

(c) Catalytic amount of molecular iodine was added to **4** in DMSO and refluxed for 4 h. TLC was done for reaction confirmation. The mixture was poured in ice cold water and ethyl acetate was used for extraction of **5**. The organic layer was washed with sodium thiosulphate solution, so that the traces of iodine get removed. Then the organic layer was filtered via drying it over sodium sulphate. The filtrate was evaporated under vacuum to get **5**.

Analytical data of representative nitro substrate, 5a (precursors of 6a). 3-(4-chlorophenyl)-5-(2-nitrophenyl)-1-phenyl-1H-pyrazole

(**5a**). Yellow solid; 89% yield; ¹H NMR (400 MHz, DMSO-*d*₆): δ 8.07 (d, *J* = 8.1 Hz, 1H), 7.97 (d, *J* = 8.5 Hz, 2H), 7.84 (t, *J* = 7.5 Hz, 1H), 7.74 (t, *J* = 7.3 Hz, 1H), 7.69 (d, *J* = 7.5 Hz, 1H), 7.54 (d, *J* = 8.5 Hz, 2H), 7.40–7.33 (m, 3H), 7.26 (d, *J* = 7.2 Hz, 2H), 7.20 (s, 1H); ¹³C NMR (100 MHz, DMSO-*d*₆): δ 150.40, 148.63, 140.12, 139.23, 134.36, 133.31, 133.18, 131.75, 131.42, 129.66, 129.36, 128.28, 127.57, 125.23, 125.11, 124.56, 106.65; MS (ESI): m/z = 375.8

General Procedure for the synthesis of 1,4-Dihydropyrazolo [4,3-*b*] indoles (6 and 7). To an oven-dried Microwave vial was added pyrazole-based nitro compound **5** (1 mmol, 1 equiv), PPh₃/P(OEt)₃ (3 equiv), and toluene (5 mL). The mixture was stirred at 180/210 °C (method A and B) in the CEM (sealed tube). After TLC indicated that **5** was consumed entirely, toluene was evaporated under vacuum, and the mixture was poured in water and extracted with ethyl acetate (25 mL). Then the solvent was evaporated under vacuum. Finally, the crude products were purified using flash column chromatography (eluent: Petroleum ether/Acetone) on silica gel to afford the desired products **6** and **7**.

Analytical data of products (6 and 7)

3-(4-chlorophenyl)-1-phenyl-1,4-dihydropyrazolo[4,3-*b*]indole (**6a**)

Compound **6a** was synthesized in accordance with the typical procedure discussed above. Purification by column chromatography on silica gel (PE/A = 19:1) afforded **6a** (60%) as a cream solid; mp: 191–193 °C; ¹H NMR (400 MHz, DMSO-*d*₆): δ 11.58 (s, 1H), 8.09 (d, *J* = 8.5 Hz, 2H), 7.91 (d, *J* = 7.8 Hz, 2H), 7.85 (d, *J* = 8.0 Hz, 1H), 7.65–7.53 (m, 5H), 7.40–7.33 (m, 2H), 7.13 (t, *J* = 7.5 Hz, 1H); ¹³C NMR (100 MHz, DMSO-*d*₆): δ 144.98, 140.76, 132.93, 132.67, 132.12, 131.54, 130.36, 130.26, 129.51, 127.73, 126.88, 125.35, 120.80, 119.51, 119.50, 113.70, 112.75; HRMS: for C₂₁H₁₄ClN₃, Exact mass: 343.0876; observed [M + H]⁺: 344.0952.

3-(4-bromophenyl)-1-phenyl-1,4-dihydropyrazolo[4,3-*b*]indole (**6b**)

Compound **6b** was synthesized in accordance with the typical procedure discussed above. Purification by column chromatography on silica gel (PE/A = 19:1) afforded **6b** (57%) as a yellow white solid; mp: 212–214 °C; ¹H NMR (400 MHz, DMSO-*d*₆): δ 11.58 (s, 1H), 8.02 (d, *J* = 8.5 Hz, 2H), 7.91 (d, *J* = 7.8 Hz, 2H), 7.85 (d, *J* = 8.0 Hz, 1H), 7.71 (d, *J* = 8.4 Hz, 2H), 7.63 (t, *J* = 7.8 Hz, 2H), 7.54 (d, *J* = 8.3 Hz, 1H), 7.40–7.33 (m, 2H), 7.13 (t, *J* = 7.5 Hz, 1H); ¹³C NMR (100 MHz, DMSO-*d*₆): δ 144.97, 140.73, 132.97, 132.39, 132.14, 131.86, 130.36, 130.24, 128.00, 126.91, 125.37, 121.23, 120.80, 119.54, 119.48, 113.70, 112.73; HRMS: for C₂₁H₁₄BrN₃, Exact mass: 387.0371; observed [M + H]⁺: 388.0436.

1-phenyl-3-(*p*-tolyl)-1,4-dihydropyrazolo[4,3-*b*]indole (**6c**)

Compound **6c** was synthesized in accordance with the typical procedure discussed above. Purification by column chromatography on silica gel (PE/A = 19:1) afforded **6c** (56%) as a light yellow solid; mp: 218–220 °C; ¹H NMR (400 MHz, DMSO-*d*₆): δ 11.50 (s, 1H), 7.97 (d, *J* = 8.1 Hz, 2H), 7.90 (d, *J* = 7.9 Hz, 2H), 7.85 (d, *J* = 8.0 Hz, 1H), 7.62 (t, *J* = 7.9 Hz, 2H), 7.54 (d, *J* = 8.3 Hz, 1H), 7.31–7.38 (m, 4H), 7.12 (t, *J* = 7.5 Hz, 1H), 2.35 (s, 3H); ¹³C NMR (100 MHz, DMSO-*d*₆): δ 144.92, 140.92, 137.66, 134.22, 131.84, 130.31, 130.03, 129.85, 126.55, 126.04, 125.13, 122.50, 120.61, 119.45, 119.37, 113.68, 112.81, 21.46; HRMS: for C₂₂H₁₇N₃, Exact Mass: 323.1422; observed [M + H]⁺: 324.1485.

3-(4-methoxyphenyl)-1-phenyl-1,4-dihydropyrazolo[4,3-*b*]indole (**6d**)

Compound **6d** was synthesized in accordance with the typical procedure discussed above. Purification by column chromatography on silica gel (PE/A = 19:1) afforded **6d** (61%) as a cream solid; mp: 221–223 °C; ¹H NMR (400 MHz, DMSO-*d*₆): δ 11.48 (s, 1H), 8.00 (d, *J* = 8.6 Hz, 2H), 7.90–7.84 (m, 3H), 7.61 (t, *J* = 7.0 Hz, 2H), 7.53 (d, *J* = 8.4 Hz, 1H), 7.37–7.31 (m, 2H), 7.14–7.06 (m, 3H), 3.81 (s, 3H); ¹³C NMR (100 MHz, DMSO-*d*₆): δ 159.53, 144.91, 140.96, 134.16, 131.79, 130.30, 130.11, 127.51, 126.41, 125.22, 125.09, 120.52, 119.47, 119.33, 114.89, 113.67, 112.85, 55.77; HRMS: for C₂₂H₁₇N₃O, Exact Mass: 339.1372; observed [M + H]⁺: 340.1452.

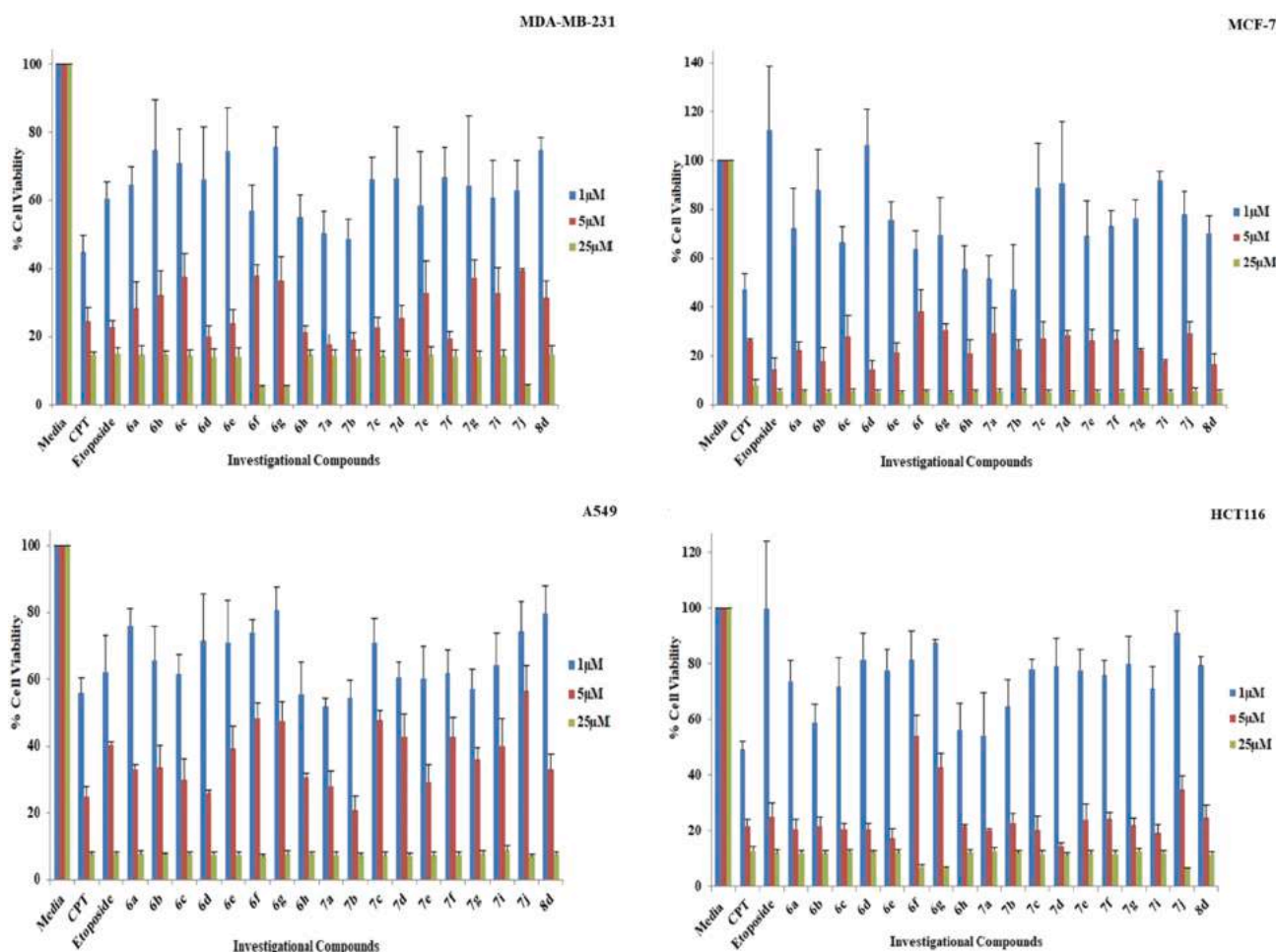


Fig. 5. *In vitro* evaluation of the antiproliferative potential of the indicated compounds in different cell lines at indicated concentrations after 24 h of treatment. Camptothecin (CPT) and etoposide were used as positive controls.

1-phenyl-3-(3,4,5-trimethoxyphenyl)-1,4-dihydropyrazolo[4,3-*b*]indole (**6e**)

Compound **6e** was synthesized in accordance with the typical procedure discussed above. Purification by column chromatography on silica gel (PE/A = 19:1) afforded **6e** (51%) as a cream solid; mp: 225–227 °C; ^1H NMR (400 MHz, $\text{DMSO}-d_6$): δ 11.5 (s, 1H), 7.9 (m, 3H), 7.7 (m, 2H), 7.6 (m, 1H), 7.4 (m, 2H), 7.3 (m, 2H), 7.2 (m, 1H), 4 (s, 6H), 3.8 (s, 3H). ^{13}C NMR (100 MHz, $\text{DMSO}-d_6$): δ 153.96, 145.01, 140.84, 139.01, 137.99, 134.23, 132.08, 130.32, 128.37, 126.70, 125.25, 122.67, 120.81, 119.46, 113.67, 112.95, 103.77, 60.70, 56.76; HRMS: for $\text{C}_{24}\text{H}_{21}\text{N}_3\text{O}_3$, Exact Mass: 399.1583; observed $[\text{M} + \text{H}]^+$: 400.1670.

1-(4-fluorophenyl)-3-(4-methoxyphenyl)-1,4-dihydropyrazolo[4,3-*b*]indole (**6f**)

Compound **6f** was synthesized in accordance with the typical procedure discussed above. Purification by column chromatography on silica gel (PE/A = 19:1) afforded **6f** (59%) as a light yellowish solid; mp: 175–176 °C; ^1H NMR (400 MHz, $\text{DMSO}-d_6$): δ 11.44 (s, 1H), 7.99 (d, J = 8.3 Hz, 2H), 7.92–7.89 (m, 2H), 7.81 (d, J = 8.0 Hz, 1H), 7.53 (d, J = 8.3 Hz, 1H), 7.45 (t, J = 8.7 Hz, 2H), 7.35–7.31 (m, 1H), 7.13–7.06 (m, 3H), 3.81 (s, 3H). ^{13}C NMR (100 MHz, $\text{DMSO}-d_6$): δ 159.54, 144.91, 137.52, 134.18, 131.88, 130.04, 127.51, 125.12, 122.55, 122.47, 119.35, 119.31, 117.21, 116.98, 114.88, 113.67, 112.71, 55.77; HRMS: for $\text{C}_{22}\text{H}_{16}\text{FN}_3\text{O}$, Exact Mass: 357.1277; observed $[\text{M} + \text{H}]^+$: 358.1371.

1-(2,4-dichlorophenyl)-3-(4-methoxyphenyl)-1,4-dihydropyrazolo[4,3-*b*]indole (**6g**)

Compound **6g** was synthesized in accordance with the typical procedure discussed above. Purification by column chromatography on

silica gel (PE/A = 19:1) afforded **6g** (54%) as a yellow solid; mp: 177–178 °C; ^1H NMR (400 MHz, $\text{DMSO}-d_6$): δ 11.42 (s, 1H), 7.98–7.75 (m, 3H), 7.74–7.63 (m, 2H), 7.49 (d, J = 8.3 Hz, 1H), 7.34–7.26 (m, 2H), 7.07–7.0 (m, 3H), 3.80 (s, 3H). ^{13}C NMR (100 MHz, $\text{DMSO}-d_6$): δ 159.60, 144.76, 137.53, 134.80, 134.51, 133.79, 130.77, 130.21, 129.18, 129.00, 127.58, 125.10, 125.02, 119.27, 119.18, 114.88, 113.47, 112.93, 55.77; HRMS: for $\text{C}_{22}\text{H}_{15}\text{Cl}_2\text{N}_3\text{O}$, Exact Mass: 407.0592; observed $[\text{M} + \text{H}]^+$: 408.0662.

3-(2,4-dimethoxyphenyl)-1-phenyl-1,4-dihydropyrazolo[4,3-*b*]indole (**6h**)

Compound **6h** was synthesized in accordance with the typical procedure discussed above. Purification by column chromatography on silica gel (PE/A = 19:1) afforded **6h** (52%) as a light yellowish solid; mp: 158–160 °C; ^1H NMR (400 MHz, $\text{DMSO}-d_6$): δ 10.35 (s, 1H), 7.88 (d, J = 7.9 Hz, 2H), 7.82 (d, J = 8.5 Hz, 2H), 7.62–7.56 (m, 3H), 7.36–7.27 (m, 2H), 7.07 (t, J = 7.6 Hz, 1H), 6.72 (d, J = 2.2 Hz, 1H), 6.66–6.63 (m, 1H), 3.94 (s, 3H), 3.81 (s, 3H). ^{13}C NMR (100 MHz, $\text{DMSO}-d_6$): δ 161.31, 158.08, 144.06, 140.96, 132.14, 131.68, 130.84, 130.25, 129.90, 126.29, 124.71, 120.68, 119.22, 118.82, 114.26, 113.78, 112.50, 106.18, 99.05, 56.66, 55.90; HRMS: for $\text{C}_{23}\text{H}_{19}\text{N}_3\text{O}_2$, Exact Mass: 369.1477; observed $[\text{M} + \text{H}]^+$: 370.1558.

3-(4-chlorophenyl)-4-ethyl-1-phenyl-1,4-dihydropyrazolo[4,3-*b*]indole (**7a**)

Compound **7a** was synthesized in accordance with the typical procedure discussed above. Purification by column chromatography on silica gel (PE/A = 99:1) afforded **7a** (21%) as a cream solid; mp: 170–172 °C; ^1H NMR (400 MHz, $\text{DMSO}-d_6$): δ 7.89–7.81 (m, 5H), 7.67–

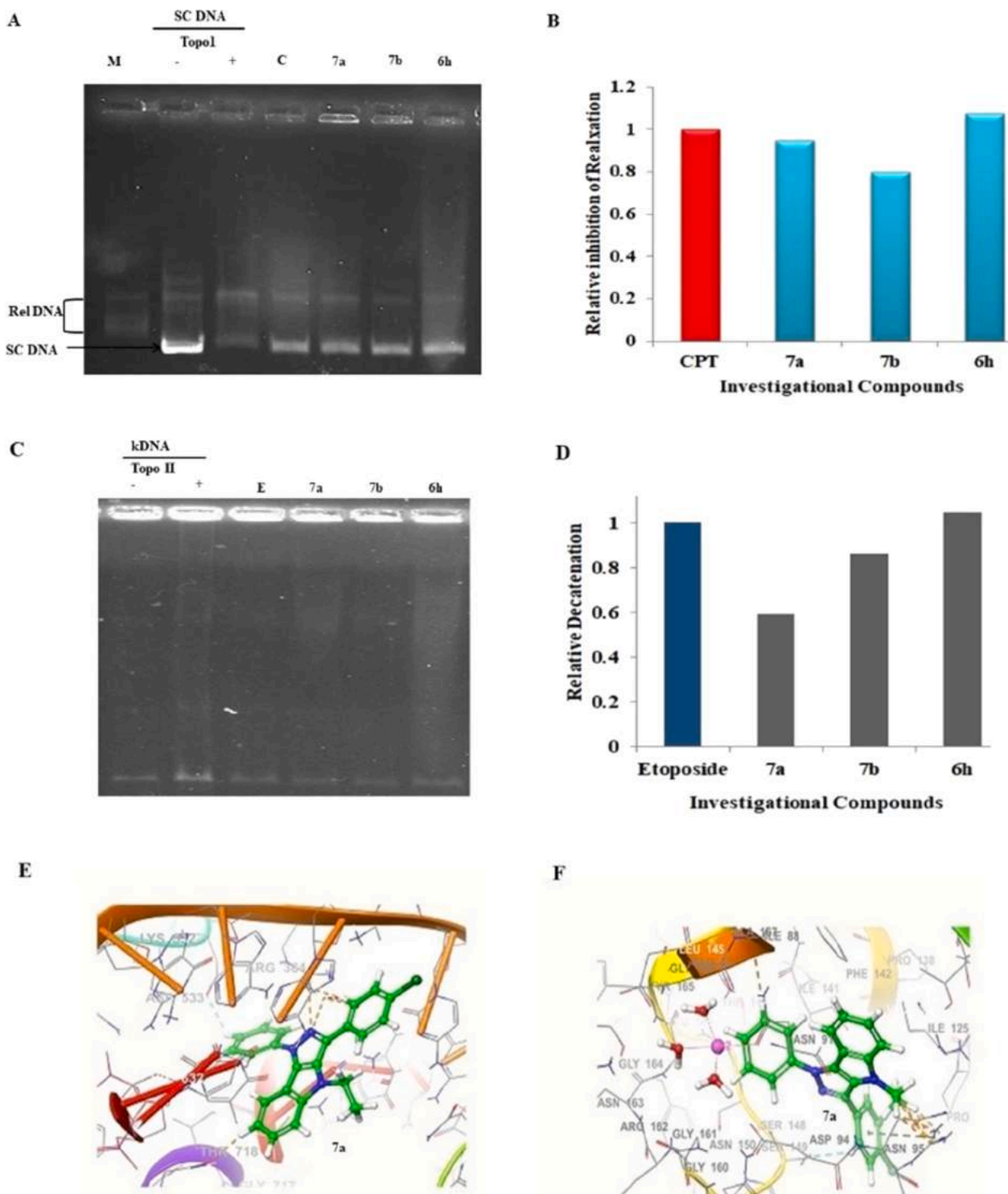


Fig. 6. A. Agarose gel image depicting the inhibition of Topo I activity B. Graph showing relative inhibition of relaxation of supercoiled DNA by compounds (100 μ M). M: Marker; C: CPT. C. Gel image showing decatenation of kDNA when treated with Topo II and its inhibition by compounds (100 μ M). D. Quantification of relative decatenation showing Topo II inhibition. E. Binding pose of **7a** with Topo I and F. Topo II active site residues.

7.58 (m, 5H), 7.39 (t, $J = 7.7$ Hz, 2H), 7.14 (t, $J = 7.5$ Hz, 1H), 4.33 (q, $J = 7.0$ Hz, 2H), 1.07 (t, $J = 7.1$ Hz, 3H); ^{13}C NMR (100 MHz, $\text{DMSO}-d_6$): δ 144.32, 140.58, 134.24, 133.38, 131.91, 131.53, 131.06, 130.49, 130.35, 129.38, 127.11, 125.46, 121.15, 119.61, 119.42, 112.60, 111.78, 40.61, 14.98; HRMS: for $\text{C}_{23}\text{H}_{18}\text{ClN}_3$, Exact Mass: 371.1189; observed $[\text{M} + \text{H}]^+$: 372.1277.

3-(4-bromophenyl)-4-ethyl-1-phenyl-1,4-dihydropyrazolo[4,3-*b*]indole (**7b**)

Compound **7b** was synthesized in accordance with the typical procedure discussed above. Purification by column chromatography on silica gel (PE/A = 99:1) afforded **7b** (22%) as a cream solid; mp: 174–176 $^{\circ}\text{C}$; ^1H NMR (400 MHz, $\text{DMSO}-d_6$): δ 7.89–7.606 (m, 10H), 7.39–7.37 (m, 2H), 7.16–7.11 (m, 1H), 4.308 (m, 2H), 1.07 (m, 3H); ^{13}C NMR (100 MHz, $\text{DMSO}-d_6$): δ 144.45, 140.58, 134.28, 132.29, 131.57, 31.03, 130.77, 130.35, 127.12, 125.48, 122.00, 121.16, 119.61, 119.43, 112.60, 111.79, 40.20, 14.98; HRMS: for $\text{C}_{23}\text{H}_{18}\text{BrN}_3$, Exact Mass:

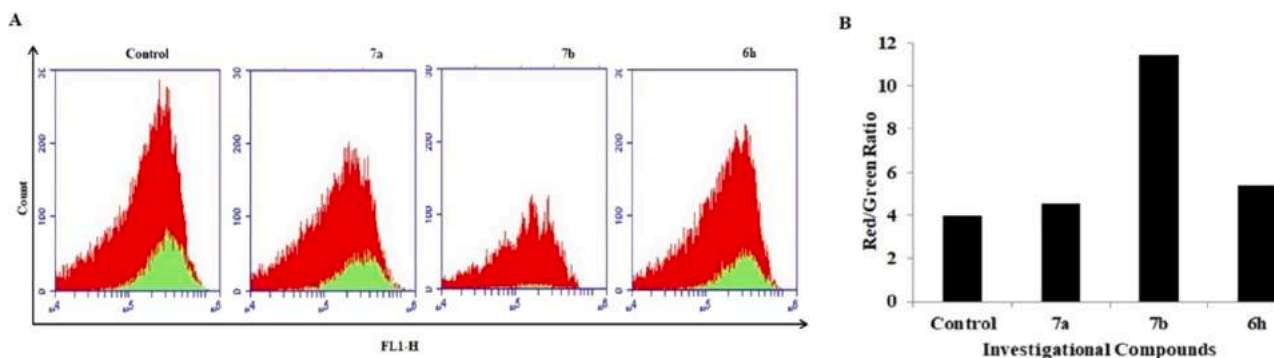


Fig. 7. A. Measurement of alteration of Mitochondrial Membrane Potential by flow cytometer. B. Ratiometric values showing the alteration in the ratio of Red (J-aggregates) to green (J-Monomer) fluorescence intensity.

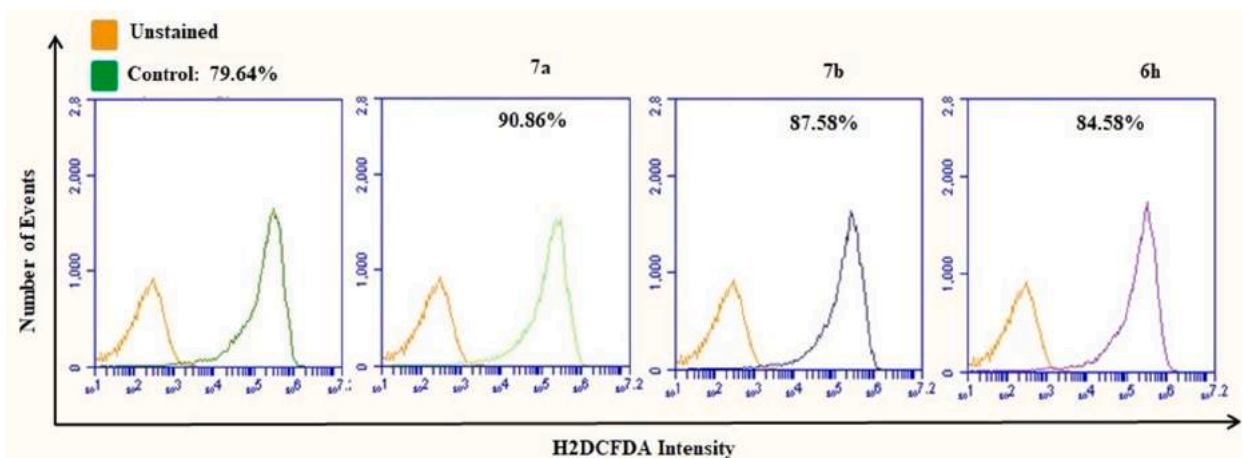


Fig. 8. Measurement of ROS alteration by flow cytometry. Compared to control, all the selected compounds could enhance ROS production at IC₅₀ values in MDA-MB-231 cells.

415.0684; observed [M + H]⁺: 416.0760.

4-ethyl-1-phenyl-3-(p-tolyl)-1,4-dihydropyrazolo[4,3-b]indole (**7c**)

Compound **7c** was synthesized in accordance with the typical procedure discussed above. Purification by column chromatography on silica gel (PE/A = 99:1) afforded **7c** (21%) as a cream solid; mp: 171–173 °C; ¹H NMR (400 MHz, DMSO-*d*₆): δ 7.88–7.83 (m, 3H), 7.69–7.59 (m, 5H), 7.39–7.32 (m, 4H), 7.13 (t, *J* = 7.5 Hz, 1H), 4.35–4.30 (m, 2H), 2.37 (s, 3H), 1.06 (t, *J* = 7.0 Hz, 3H); ¹³C NMR (100 MHz, DMSO-*d*₆): δ 144.22, 140.73, 138.05, 135.57, 131.25, 131.19, 130.31, 130.14, 129.87, 128.72, 126.83, 125.28, 120.99, 119.60, 119.29, 112.69, 111.75, 40.63, 21.44, 14.99; HRMS: for C₂₄H₂₁N₃, Exact Mass: 351.1735; observed [M + H]⁺: 352.1831.

4-ethyl-3-(4-methoxyphenyl)-1-phenyl-1,4-dihydropyrazolo[4,3-b]indole (**7d**)

Compound **7d** was synthesized in accordance with the typical procedure discussed above. Purification by column chromatography on silica gel (PE/A = 99:1) afforded **7d** (18%) as a cream solid; mp: 152–154 °C; ¹H NMR (400 MHz, DMSO-*d*₆): δ 7.88–7.83 (m, 3H), 7.74–7.70 (m, 2H), 7.64–7.59 (m, 3H), 7.40–7.35 (m, 2H), 7.15–7.07 (m, 3H), 4.35–4.30 (m, 2H), 3.81 (s, 3H), 1.07 (t, *J* = 7.1 Hz, 3H); ¹³C NMR (100 MHz, DMSO-*d*₆): δ 159.76, 144.18, 140.76, 135.43, 131.16, 130.30, 130.12, 126.73, 125.31, 125.24, 120.91, 119.61, 119.26, 114.70, 112.70, 111.72, 55.73, 40.67, 15.01; HRMS: for C₂₄H₂₁N₃O, Exact Mass: 367.1685; observed [M + H]⁺: 368.1761.

4-ethyl-1-phenyl-3-(3,4,5-trimethoxyphenyl)-1,4-dihydropyrazolo[4,3-b]indole (**7e**)

Compound **7e** was synthesized in accordance with the typical procedure discussed above. Purification by column chromatography on

silica gel (PE/A = 99:1) afforded **7e** (20%) as a cream yellow; mp: 138–140 °C; ¹H NMR (400 MHz, DMSO-*d*₆): δ 8 (d, *J* = 8.7 Hz, 1H), 7.93–7.87 (m, 2H), 7.74 (d, *J* = 8.8 Hz, 1H), 7.69–7.64 (m, 2H), 7.44–7.42 (m, 2H), 7.17 (m, 1H), 7.09 (d, *J* = 4 Hz, 2H), 4.42–4.40 (m, 2H), 3.8 (s, 6H), 3.75 (s, 3H), 1.25–1.20 (m, 3H); ¹³C NMR (100 MHz, DMSO-*d*₆): δ 153.60, 144.13, 140.69, 139.03, 135.55, 131.21, 130.33, 128.58, 126.93, 125.32, 122.97, 121.12, 119.59, 119.29, 112.55, 111.73, 106.07, 60.69, 56.51, 40.62, 15.12; HRMS: for C₂₆H₂₅N₃O₃, Exact Mass: 427.1896; observed [M + H]⁺: 428.1967.

4-ethyl-1-(4-fluorophenyl)-3-(4-methoxyphenyl)-1,4-dihydropyrazolo[4,3-b]indole (**7f**)

Compound **7f** was synthesized in accordance with the typical procedure discussed above. Purification by column chromatography on silica gel (PE/A = 99:1) afforded **7f** (22%) as a cream solid; mp: 158–159 °C; ¹H NMR (400 MHz, DMSO-*d*₆): δ 7.90–7.87 (m, 2H), 7.80 (d, *J* = 8.1 Hz, 1H), 7.71 (d, *J* = 8.5 Hz, 2H), 7.62 (d, *J* = 8.4 Hz, 1H), 7.44 (t, *J* = 8.7 Hz, 3H), 7.14–7.07 (m, 3H), 4.34–4.29 (m, *J* = 7.0 Hz, 2H), 3.81 (s, 3H), 1.07 (m, 3H). ¹³C NMR (100 MHz, DMSO-*d*₆): δ 161.91, 159.78, 144.20, 137.32, 135.43, 131.28, 131.07, 130.10, 125.25, 122.99, 122.91, 119.50, 119.25, 117.22, 116.99, 114.71, 112.57, 111.72, 55.73, 40.65, 15.00.

1-(2,4-dichlorophenyl)-4-ethyl-3-(4-methoxyphenyl)-1,4-dihydropyrazolo[4,3-b]indole (**7g**)

Compound **7g** was synthesized in accordance with the typical procedure discussed above. Purification by column chromatography on silica gel (PE/A = 99:1) afforded **7g** (22%) as a cream solid; mp: 124–125 °C; ¹H NMR (400 MHz, DMSO-*d*₆): δ 7.94 (d, *J* = 2.2 Hz, 1H), 7.76–7.58 (m, 5H), 7.34–7.31 (m, 2H), 7.09–7.02 (m, 3H), 4.35–4.30

(m, 2H), 3.8(s, 3H), 1.12–1.08 (m, 3H). ^{13}C NMR (100 MHz, DMSO- d_6) δ 159.81, 144.04, 137.26, 135.93, 133.96, 133.77, 130.82, 130.23, 130.08, 129.99, 129.20, 125.19, 125.14, 119.38, 119.23, 114.74, 112.65, 111.54, 55.73, 39.49, 15.20.

4-ethyl-3-(3-iodo-4-methoxyphenyl)-1-phenyl-1,4-dihydropyrazolo[4,3-*b*]indole (**7i**)

Compound **7i** was synthesized in accordance with the typical procedure discussed above. Purification by column chromatography on silica gel (PE/A = 99:1) afforded **7i** (41%) as a cream solid; mp: 173–175 °C; ^1H NMR (400 MHz, DMSO- d_6): δ 8.16–8.18 (m, 1H), 7.94 (d, J = 8.6 Hz, 1H), 7.88–7.77 (m, 3H), 7.69 (d, J = 8.6 Hz, 1H), 7.64–7.59 (m, 2H), 7.38 (t, J = 7.0 Hz, 2H), 7.16–7.11 (m, 2H), 4.32–4.28 (m, 2H), 3.88 (s, 3H), 1.13–1.08 (m, 3H); ^{13}C NMR (100 MHz, DMSO- d_6): δ 158.36, 144.22, 140.30, 139.01, 138.93, 134.34, 130.33, 130.15, 127.03, 125.48, 122.94, 121.06, 119.79, 119.62, 112.53, 112.11, 111.73, 91.54, 86.95, 57.06, 40.67, 15.05; HRMS: for $\text{C}_{24}\text{H}_{20}\text{IN}_3\text{O}$, Exact Mass: 493.0651; observed $[\text{M} + \text{H}]^+$: 494.0714.

4-ethyl-3-(naphthalen-2-yl)-1-phenyl-1,4-dihydropyrazolo[4,3-*b*]indole (**7j**)

Compound **7j** was synthesized in accordance with the typical procedure discussed above. Purification by column chromatography on silica gel (PE/A = 99:1) afforded **7j** (48%) as a white solid; mp: 177–179 °C; ^1H NMR (400 MHz, DMSO- d_6): δ 8.34 (s, 1H), 8.07–8.04 (m, 2H), 7.99–7.92 (m, 4H), 7.90–7.86 (m, 1H), 7.75 (d, J = 8.7 Hz, 1H), 7.69–7.62 (m, 2H), 7.58–7.53 (m, 2H), 7.42–7.38 (m, 2H), 7.18–7.14 (m, 1H), 4.44–4.41 (m, 2H), 1.10–1.05 (m, 3H). ^{13}C NMR (100 MHz, DMSO- d_6): δ 144.40, 140.70, 139.06, 133.51, 133.04, 131.53, 130.49, 130.36, 128.83, 128.70, 128.25, 127.60, 127.50, 127.20, 127.01, 126.79, 125.41, 122.99, 121.13, 119.64, 119.41, 112.72, 111.82, 40.62, 15.02; HRMS: for $\text{C}_{22}\text{H}_{21}\text{N}_3$, Exact Mass: 388.1805; observed $[\text{M} + \text{H}]^+$: 388.1801.

General Procedure for the synthesis of 8d in-situ benzylation. To an oven-dried Microwave vial was added **5d** (1 mmol, 1 equiv), PPh_3 (3 equiv), benzyl chloride (1.5 equiv) and toluene (5 mL). The mixture was stirred at 180 °C in the CEM (sealed tube) for 20 min. After TLC indicated that **5d** was completely consumed. Toluene was evaporated under vacuum, and the mixture was poured in water and extracted with ethyl acetate (25 mL). Then the solvent was evaporated under vacuum. The crude product was purified using flash column chromatography (eluent: Petroleum ether/Acetone) on silica gel to afford the desired product **8d**. Cream solid; Purification by column chromatography on silica gel (PE/A = 19:1): 61% yield; mp: 140–142 °C; ^1H NMR (500 MHz, DMSO- d_6): δ 7.92–7.95 (m, 3H), 7.69–7.64 (m, 5H), 7.45–7.38 (m, 2H), 7.20 (d, J = 8.6 Hz, 4H), 7.04 (d, J = 10.4 Hz, 2H), 6.94 (d, J = 8.5 Hz, 2H), 5.56 (s, 2H), 3.82 (s, 3H); ^{13}C NMR (125 MHz, DMSO- d_6): δ 159.74, 144.71, 140.66, 138.12, 135.43, 131.62, 131.24, 130.27, 130.15, 129.07, 127.78, 126.78, 126.76, 125.38, 125.05, 120.91, 119.63, 119.62, 114.62, 112.87, 112.17, 55.69, 47.75; HRMS: for $\text{C}_{29}\text{H}_{23}\text{N}_3\text{O}$, Exact Mass: 429.1841; observed $[\text{M} + \text{H}]^+$: 430.1920.

Procedure for controlled experiments. To gather more pieces of evidence in favor of the nitrene pathway, we set a controlled experiment (Scheme S2) where a reaction of **5d** (1 equiv) with triethyl phosphite (3 equiv) was carried out in toluene as solvent. The reaction mixture was refluxed for 4 h, and the sample was collected from the reaction mixture for LCMS analysis.

5. Biology

5.1. Cell lines and cell culture

Cell lines (MDA-MB-231, MCF-7, A549, and HCT-116) were procured from National Centre for Cell Science (NCCS) Pune, India and maintained per instructions in DMEM media mixed with 10% FBS, 1% Penicillin-Streptomycin solution in a CO_2 incubator. Upon reaching 80% confluency, they were passaged with the help of 0.25% Trypsin-EDTA solution (Gibco) and were further utilized according to the

experimental setup.

Human peripheral blood mononuclear cells (hPBMCs) were isolated from healthy individuals. RBCs were lysed in lysis buffer, and the hPBMCs were cultured in RPMI media and treated accordingly with the compounds as discussed below to assess the selectivity of investigational compounds toward cancer cells. The assay was performed strictly as per protocol no. CUPB/cc/14/IEC/4483 approved by Institutional Ethics Committee of Central University of Punjab, Bathinda, and according to the Indian Council of Medical Research (ICMR) guidelines Govt. of India.

5.2. Evaluation of antiproliferative potential of synthesized compounds by 3-(4,5-dimethylthiazol-2-yl)-2,5-diphenyl tetrazolium bromide (MTT) assay

The antiproliferative potential of the investigational compounds was assessed using MTT assay (Invitrogen) in different cells. 7×10^3 cells were seeded in a 96-well plate. The following day, cells were serum-starved, and synthetic compounds were treated and incubated for 24 h following which 10 μL of MTT dye (5 mg/mL of 1X PBS) was added to each well and incubated in CO_2 atmosphere in the dark for 4 h to allow formazan crystals formation. 100 μL DMSO (100%) was added to each well, and absorbance was read using a microplate reader at 570 nm. % cell viability was calculated using the formula given below, and IC_{50} values were calculated using ORIGIN software.

$$\% \text{ Cell Viability} = \text{OD}_{\text{Test Compound}} / \text{OD}_{\text{Media (Control)}} * 100$$

5.3. Topoisomerase assay

Topoisomerase I (Catalogue No TG2005H-RC) and Topoisomerase II (Catalogue No TG2000H-1) assay kits were procured from Topogen (Topogen, Inc. Buena Vista, CO, USA). DNA relaxation and DNA decatenation assays were performed as per the manufacturer's instructions. Negatively supercoiled DNA (SC DNA) and camptothecin (CPT) were used as substrate and positive control. The total reaction mixture was incubated at 37 °C for 30 min and stopped by the addition of 2 μL 10% SDS. The samples were run on 0.8% agarose gel for 1–2 h at 50 V and then stained with the help of EtBr for 15 min followed by destaining in water, and images were recorded in Chemi-DocTM XRS+ (Bio-Rad). For topoisomerase-II, kinetoplast DNA (kDNA) acted as substrate and etoposide, an inhibitor of Topo II, was used as a positive control as described previously.[47]

5.4. Molecular docking studies

The ligand-bound crystal structures of human topoisomerase I and II (PDB ID's: 1T8I [48] and 4R1F [49]) were imported from Protein Data Bank (www.rcsb.org) in Schrödinger (2020–4). Both the proteins were prepared using protein preparation wizard in Maestro 12.6. The binding cavity was defined using receptor grid generation, and the grid was generated around the already bound ligand. All the synthesized ligands were drawn using ChemDraw Professional in 2D format and saved in 'sdf' format. All the ligands were prepared using the LIGPREP module in a 3D format using the OPLS3 force field. All the prepared ligands were docked at the topoisomerase I and II binding sites using the GLIDE module in Maestro 12.6. The result revealed the affinity and binding interactions of ligands with the proteins. The docking scores were generated.[50]

5.5. Mitochondrial membrane potential (MMP) and reactive oxygen species (ROS) assay

To assess MMP and ROS level alteration induced by compounds, cells were plated in 100 mm culture dishes and treated with chosen compounds at their respective IC_{50} values for 24 h. The pellets were washed twice with the help of sterile 1X PBS (Gibco). The MMP in MDA-MB-231

cells was monitored using incubation of JC-1 (Life Technologies, Thermo Fisher Scientific), an MMP-sensitive fluorescent dye, with resuspended cell pellet for 30 min at 37 °C and analyzed using a flow cytometer (BD Biosciences, San Jose, CA, USA).

Declaration of Competing Interest

The authors declare that they have no known competing financial interests or personal relationships that could have appeared to influence the work reported in this paper.

Acknowledgements

MK thanks the DST-Inspire, New Delhi (IF 180460), for providing the JRF. MK and RK are thankful to Professor R. P. Tiwari, Vice-Chancellor, to support the present work. RK thanks SERB (EMR/2017/002702), Delhi, for financial support. The authors also thank CIL, CUPB, and DST-FIST (for GC-MS) support to the department for data analysis and CIF, BIT Mesra for X-ray diffraction data collection.

Appendix A. Supplementary material

The Supplementary data includes copies of ^1H and ^{13}C NMR spectra, HRMS spectra, LCMS spectra, X-ray crystallographic data (Figure S1) and other figures (such as docking images and drug response curves) (S2-S7) and Schemes. Supplementary data to this article can be found online at <https://doi.org/10.1016/j.bioorg.2021.105114>.

References

- [1] M. Kaur, R. Kumar, C-N and N-N bond formation via Reductive Cyclization: Progress in Cadogan/Cadogan-Sundberg Reaction, *ChemistrySelect* 3 (19) (2018) 5330–5340.
- [2] S. Sinha, R. Sikari, V. Sinha, U. Jash, S. Das, P. Brandão, S. Demeshko, F. Meyer, B. de Bruin, N.D. Paul, Iron-Catalyzed/Mediated C-N Bond Formation: Competition between Substrate Amination and Ligand Amination, *Inorg. Chem.* 58 (3) (2019) 1935–1948.
- [3] J. Bariwal, E. Van der Eycken, C-N bond forming cross-coupling reactions: an overview, *Chem. Soc. Rev.* 42 (2013) 9283–9303.
- [4] Ali, I., Nadeem Lone, M., A Al-Othman, Z., Al-Warthan, A., Marsin Sanagi, M., Heterocyclic scaffolds: centrality in anticancer drug development, *Curr. Drug Targets* 16(7) (2015) 711–734.
- [5] L. Zou, X. Duan, W. Zhou, H. Zhang, S. Chen, J. Chai, X. Liu, L. Shen, J. Xu, G. Zhang, Electrochemical capacitive performance of free-standing polyindole film and effect of introducing alkyl chain connecting two indoles, *J. Mater. Sci.: Mater. Electron.* 1–8 (2019).
- [6] C. Lamberth, Heterocyclic chemistry in crop protection, *Pest Manage. Sci.* 69 (10) (2013) 1106–1114.
- [7] S. Urgaonkar, J.G. Verkade, Scope and limitations of Pd2 (dba) 3/P (i-BuNCH2CH2) 3N-catalyzed Buchwald–Hartwig amination reactions of aryl chlorides, *J. Org. Chem.* 69 (26) (2004) 9135–9142.
- [8] V. Gracias, J.D. Moore, S.W. Djuric, Sequential Ugi/Heck cyclization strategies for the facile construction of highly functionalized N-heterocyclic scaffolds, *Tetrahedron Lett.* 45 (2) (2004) 417–420.
- [9] T. Rosenau, A. Potthast, J. Roehrling, A. Hofinger, H. Sixta, P. Kosma, A solvent-free and formalin-free Eschweiler-Clarke methylation for amines, *Synth. Comm.* 32 (3) (2002) 457–466.
- [10] Merisor, E., Synthesis of N-heterocycles via intramolecular reductive cyclizations of nitroalkenes, (2008).
- [11] Lu, C., Su, Z., Jing, D., Jin, S., Xie, L., Li, L., Zheng, K., Intramolecular Reductive Cyclization of o-Nitroarenes via Biradical Recombination, *Org. Lett.* (2019).
- [12] H. Peng, X. Chen, Y. Chen, Q. He, Y. Xie, C. Yang, Solvent-free synthesis of δ -carboline/carbazoles from 3-nitro-2-phenylpyridines/2-nitrobiphenyl derivatives using DPPE as a reducing agent, *Tetrahedron* 67 (32) (2011) 5725–5731.
- [13] J.S. Zhu, C.J. Li, K.Y. Tsui, N. Kraemer, J.-H. Son, M.J. Haddadin, D.J. Tantillo, M. J. Kurth, Accessing Multiple Classes of 2H-Indazoles: Mechanistic Implications for the Cadogan and Davis-Beirut Reactions, *J. Am. Chem. Soc.* 2019.
- [14] M. Shevlin, X. Guan, T.G. Driver, Iron-catalyzed reductive cyclization of O-nitrostyrenes using phenylsilane as the terminal reductant, *ACS Catalysis* 7 (8) (2017) 5518–5522.
- [15] P. Bunyan, J. Cadogan, 7. The reactivity of organophosphorus compounds. Part XIV. Deoxygenation of aromatic C-nitroso-compounds by triethyl phosphite and triphenylphosphine: a new cyclization reaction, *J. Chem. Soc.* (1963) 42–49.
- [16] R. Sundberg, Deoxygenation of nitro groups by trivalent phosphorus. Indoles from o-nitrostyrenes, *J. Org. Chem.* 30 (11) (1965) 3604–3610.
- [17] P. Bhutani, G. Joshi, N. Raja, N. Bachhav, P.K. Rajanna, H. Bhutani, A.T. Paul, R. Kumar, US FDA approved drugs from 2015–June 2020: a perspective, *J. Med. Chem.* 64 (5) (2021) 2339–2381.
- [18] C. Sawyers, Targeted cancer therapy, *Nature* 432 (7015) (2004) 294–297.
- [19] J.L. Delgado, C.-M. Hsieh, N.-L. Chan, H. Hiasa, Topoisomerases as anticancer targets, *Biochem. J.* 475 (2) (2018) 373–398.
- [20] M. Westphal, C.L. Maire, K. Lamszus, EGFR as a target for glioblastoma treatment: an unfulfilled promise, *CNS drugs* 31 (9) (2017) 723–735.
- [21] C. Zhao, H. Dong, Q. Xu, Y. Zhang, Histone deacetylase (HDAC) inhibitors in cancer: a patent review (2017–present), *Expert Opin. Ther. Pat.* 30 (4) (2020) 263–274.
- [22] F. You, C. Gao, Topoisomerase inhibitors and targeted delivery in cancer therapy, *Curr. Top. Med. Chem.* 19 (9) (2019) 713–729.
- [23] Y. Wan, Y. Li, C. Yan, M. Yan, Z. Tang, Indole: A privileged scaffold for the design of anti-cancer agents, *Eur. J. Med. Chem.* 183 (2019), 111691.
- [24] N. Chadha, O. Silakari, Indoles: As Multitarget Directed Ligands in Medicinal Chemistry, Elsevier, Key Heterocycle Cores for Designing Multitargeting Molecules, 2018, pp. 285–321.
- [25] A.B. Smith, A.H. Davulcu, L. Kürti, Indole Diterpenoid Synthetic Studies. Construction of the Heptacyclic Core of (–)-Nodulisporic Acid D, *Org. Lett.* 8 (8) (2006) 1669–1672.
- [26] N. Chadha, O. Silakari, Indoles as therapeutics of interest in medicinal chemistry: Bird's eye view, *Eur. J. Med. Chem.* 134 (2017) 159–184.
- [27] S. Issa, A. Prandina, N. Bedel, P. Rongved, S. Yous, M. Le Borgne, Z. Bouaziz, Carbazole scaffolds in cancer therapy: a review from 2012 to 2018, *J. Enzyme Inhib. Med. Chem.* 34 (1) (2019) 1321–1346.
- [28] J.M. Alex, R. Kumar, 4, 5-Dihydro-1 H-pyrazole: an indispensable scaffold, *J. Enzyme Inhib. Med. Chem.* 29 (3) (2014) 427–442.
- [29] G. Joshi, S.M. Amrutkar, A.T. Baviskar, H. Kler, S. Singh, U.C. Banerjee, R. Kumar, Synthesis and biological evaluation of new 2, 5-dimethylthiophene/furan based N-acetyl pyrazolines as selective topoisomerase II inhibitors, *RSC Adv.* 6 (18) (2016) 14880–14892.
- [30] S. Kumar, H. Ila, H. Junjappa, Efficient Routes to Pyrazolo [3, 4-b] indoles and Pyrazolo [1, 5-a] benzimidazoles via Palladium-and Copper-Catalyzed Intramolecular C–C and C–N Bond Formation, *J. Org. Chem.* 74 (18) (2009) 7046–7051.
- [31] Z. Hou, S. Oishi, Y. Suzuki, T. Kure, I. Nakanishi, A. Hirasawa, G. Tsujimoto, H. Ohno, N. Fujii, Diversity-oriented synthesis of pyrazolo [4, 3-b] indoles by gold-catalyzed three-component annulation: application to the development of a new class of CK2 inhibitors, *Org. Biomol. Chem.* 11 (20) (2013) 3288–3296.
- [32] H. Liu, L. Zhang, F. Zhao, H. Liu, Three-Step One-Pot Synthesis of 1, 4-Dihydro-pyrazolo [4, 3-b] indoles Using Copper Catalysis, *Eur. J. Org. Chem.* 2014 (5) (2014) 1047–1052.
- [33] J.M. Alex, S. Singh, R. Kumar, 1-Acetyl-3, 5-diaryl-4, 5-dihydro (1H) pyrazoles: exhibiting anticancer activity through intracellular ROS scavenging and the mitochondria-dependent death pathway, *Arch. Pharm.* 347 (10) (2014) 717–727.
- [34] C.O. Kappe, Microwave dielectric heating in synthetic organic chemistry, *Chem. Soc. Rev.* 37 (6) (2008) 1127–1139.
- [35] M. Frisch, G. Trucks, H. Schlegel, G. Scuseria, M. Robb, J. Cheeseman, G. Scalmani, V. Barone, B. Mennucci, G. Petersson, Gaussian 09, Gaussian Inc, Wallingford, CT, 2009.
- [36] C. Lee, W. Yang, R. Parr, Density-functional exchange-energy approximation with correct asymptotic behaviour, *Phys. Rev. B* 37 (1988) 785–789.
- [37] C. Lee, W. Yang, R.G. Parr, Development of the Colle-Salvetti correlation-energy formula into a functional of the electron density, *Phys. Rev. B* 37 (2) (1988) 785.
- [38] R.J. Sundberg, T. Yamazaki, Rearrangements and ring expansions during the deoxygenation of beta., beta.-disubstituted o-nitrostyrenes, *J. Org. Chem.* 32 (2) (1967) 290–294.
- [39] R. Sundberg, A Study of the Deoxygenation of Some o-Alkylnitro-and o-Alkylnitrosobenzenes in Triethyl Phosphite, *J. Am. Chem. Soc.* 88 (16) (1966) 3781–3789.
- [40] N. Ono, The Nitro-Aldol (Henry) Reaction, *The Nitro Group in Organic, Synthesis* (2001) 30–69.
- [41] G.W. Gribble, Recent developments in indole ring synthesis—methodology and applications, *J. Chem. Soc., Perkin Trans 1* (7) (2000) 1045–1075.
- [42] H. Majgier-Baranowska, J.D. Williams, B. Li, N.P. Peet, Studies on the mechanism of the Cadogan-Sundberg indole synthesis, *Tetrahedron Lett.* 53 (35) (2012) 4785–4788.
- [43] I.T. Alt, B. Plietker, Iron-Catalyzed Intramolecular C (sp²)–H Amination, *Angew. Chem.* 55 (4) (2016) 1519–1522.
- [44] I.W. Davies, V.A. Guner, K. Houk, Theoretical evidence for oxygenated intermediates in the reductive cyclization of nitrobenzenes, *Org. Lett.* 6 (5) (2004) 743–746.
- [45] C.R. Reczek, N.S. Chandel, The two faces of reactive oxygen species in cancer, *Annu. Rev. Cancer Biol.* 1 (2017) 79–98.
- [46] S. Marchi, C. Giorgi, J.M. Suski, C. Agnoletto, A. Bononi, M. Bonora, E. De Marchi, S. Missiroli, S. Patergnani, F. Poletti, Mitochondria-ros crosstalk in the control of cell death and aging, *J. Signal Transduct.* 2012 (2012), 329635.
- [47] G. Joshi, S. Kalra, U.P. Yadav, P. Sharma, P.K. Singh, S. Amrutkar, A.J. Ansari, S. Kumar, A. Sharon, S. Sharma, E-pharmacophore guided discovery of pyrazolo [1, 5-c] quinoxalines as dual inhibitors of topoisomerase-I and histone deacetylase, *Bioorg. Chem.* 94 (2020), 103409.

- [48] B.L. Staker, M.D. Feese, M. Cushman, Y. Pommier, D. Zembower, L. Stewart, A. B. Burgin, Structures of three classes of anticancer agents bound to the human topoisomerase I– DNA covalent complex, *J. Med. Chem.* 48 (7) (2005) 2336–2345.
- [49] F.V. Stanger, C. Dehio, T. Schirmer, Structure of the N-terminal gyrase B fragment in complex with ADP· P_i reveals rigid-body motion induced by ATP hydrolysis, *PLoS one* 9 (9) (2014), e107289.
- [50] S. Arora, G. Joshi, S. Kalra, A.A. Wani, P.V. Bharatam, P. Kumar, R. Kumar, Knoevenagel/tandem knoevenagel and michael adducts of cyclohexane-1, 3-dione and aryl aldehydes: synthesis, DFT studies, xanthine oxidase inhibitory potential, and molecular modeling, *Acs Omega* 4 (3) (2019) 4604–4614.

ChemComm

Accepted Manuscript



This article can be cited before page numbers have been issued, to do this please use: D. M. Sawant, S. Sharma, R. S. Pathare, G. Joshi, S. Kalra, S. Sukanya, A. K. Maurya, R. K. Metre, V. K. Agnihotri, S. Khan, R. Kumar and R. T. Pardasani, *Chem. Commun.*, 2018, DOI: 10.1039/C8CC05845H.



This is an Accepted Manuscript, which has been through the Royal Society of Chemistry peer review process and has been accepted for publication.

Accepted Manuscripts are published online shortly after acceptance, before technical editing, formatting and proof reading. Using this free service, authors can make their results available to the community, in citable form, before we publish the edited article. We will replace this Accepted Manuscript with the edited and formatted Advance Article as soon as it is available.

You can find more information about Accepted Manuscripts in the [author guidelines](#).

Please note that technical editing may introduce minor changes to the text and/or graphics, which may alter content. The journal's standard [Terms & Conditions](#) and the ethical guidelines, outlined in our [author and reviewer resource centre](#), still apply. In no event shall the Royal Society of Chemistry be held responsible for any errors or omissions in this Accepted Manuscript or any consequences arising from the use of any information it contains.



Journal Name

COMMUNICATION

Relay Tricyclic Pd(II)/Ag(I) Catalysis: Design of a Four-Component Reaction Driven by Nitrene-Transfer on Isocyanide Yields Inhibitors of EGFR

Received 00th January 20xx,
Accepted 00th January 20xx

DOI: 10.1039/x0xx00000x

www.rsc.org/

One-pot synthesis of pyrazolo[1,5-c]quinazolines from four easily available precursors is presented through a one-pot tricyclic Pd(II)/Ag(I) relay catalysis. The bimetallic relay cascade forges five new chemical bonds by concatenating six discrete chemical steps. The relay catalysis enables four-component assembly of pyrazolo[1,5-c]quinazolines that selectively inhibit EGFR, exhibit apoptosis through the ROS-induced mitochondrial-mediated pathway, and arrest the cell cycle at G1 phase.

One of the important objectives of synthetic organic chemistry is to design rapid, efficient and sustainable strategies to access valuable molecular constructs. To this end, chemists have designed tandem or cascade reactions that generate complex molecular frameworks in one-pot without the need for any isolation of an intermediate.¹ Recently, there is an upsurge in the field of organic synthesis for the development of catalytic multistep processes, whereby two or more distinct chemical transformations are promoted by more than one catalysts in a single flask. Classified as cooperative-,² synergistic-,³ relay-⁴ or sequential-catalysis⁵ depending on the precise experimental details offers the potential for the advancement in the synthesis by removing dependency over iterative processes.⁶ Of these, orthogonal relay catalyses of transition-metals, where all metal catalysts are present at the outset, are somewhat difficult to design owing to the redox incompatibilities among various metals and a challenging time-resolution of such methods (Fig. 1). Besides, among various methods reported so far, the second transition metal is often

employed as a redox⁷ or photoredox⁸ partner in the majority of these reports, which doesn't expand the overall range of transformations. In 2011, Lautens reported relay catalysis of Rh-catalyzed alkyne arylation and Pd-catalyzed N-arylation steps for the synthesis of dihydroquinolines [Eq.(1)].^{9,10} Tu employed Co(II)/Ag(I) relay catalysis in 2015 for isocyanide insertion/cycloaddition cascade to access a new pyrrolo[2,3-b]indole heterocycle [Eq.(2)].¹¹ Ji reported Rh(II)/Pd(0) dual catalysis for selective construction of cyclic quarternary carbon center [Eq.(3)]¹² and Ramasastry developed trimetallic relay catalysis for the synthesis of β -carbolines in 2016 [Eq.(4)].¹³ In 2017, Wang successfully applied Rh(III)/Ag(I) relay catalysis in the total synthesis of aristolactam BII¹⁴ [Eq.(5)] and Xu

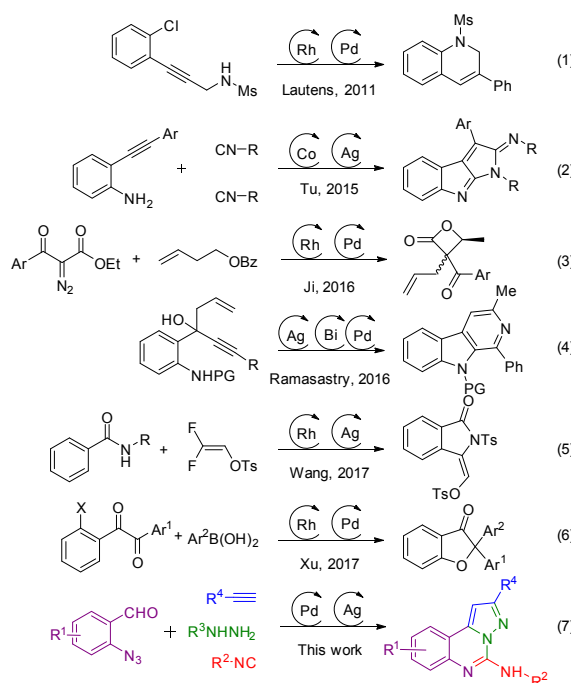


Fig. 1. Various strategies reported for relay catalysis promoted by two or more transition metal catalysts.

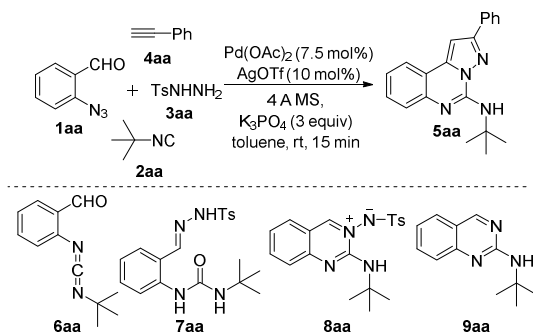
Electronic Supplementary Information (ESI) available: [details of any supplementary information available should be included here]. See DOI: 10.1039/x0xx00000x

COMMUNICATION

reported rhodium/palladium relay catalysis for enantioselective synthesis of gem-diaryl benzofuran-3(2H)-ones [Eq.(6)].¹⁵ In spite of their utility, all methodologies of bimetallic relay catalysis relied on the requirement of prefabricated substrates synthesized by convergent multistep routes. However, the cutting-edge application of multicatalytic relay catalysis lies in promoting multicomponent reactions, since it imitates a biological process where several enzymes coordinate to generate complex molecular frameworks from multiple, simple and easily available starting materials.¹⁶ To our surprise, multicomponent relay catalysis of two or more transition metals received scant synthetic attention.¹¹ As a consequence, the scope of the bimetallic relay catalysts is limited, and its true potential for promoting the multicomponent reaction has not been explored to date.

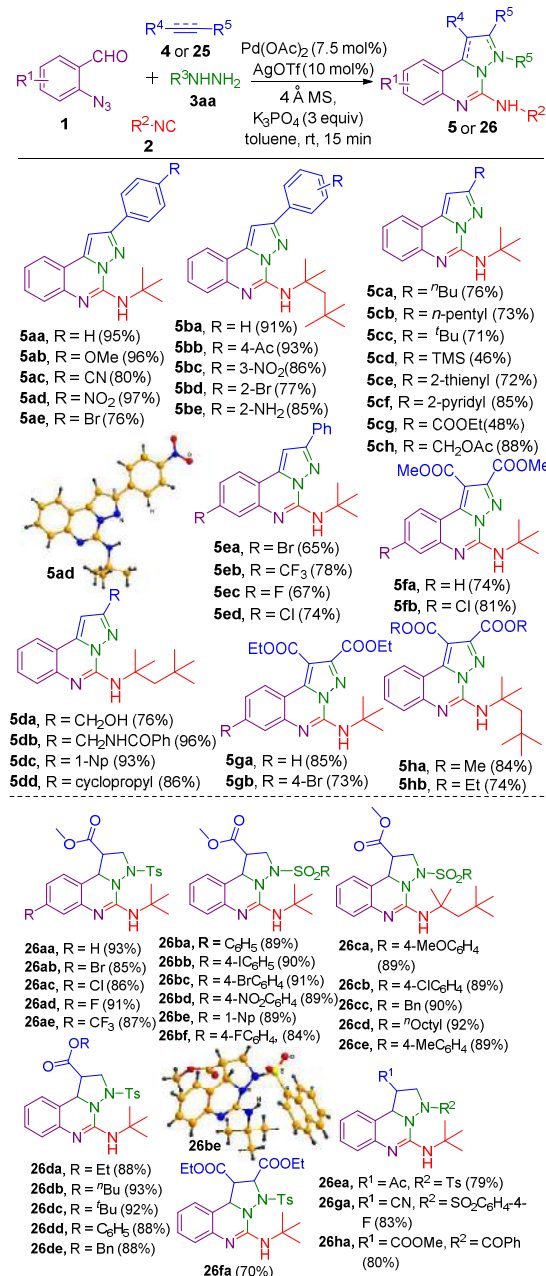
We now report a four component reaction (4-CR) employing four versatile privileged synthons: 2-azidobenzaldehyde, isocyanide, sulfonyl hydrazides and alkynes promoted by two different transition metal catalyst in a time-resolved manner, thus leading to an efficient preparation of pharmacologically active pyrazolo[1,5-c]quinazolines.¹⁷ The corresponding focused compound collection of pyrazolo[1,5-c]quinazolines exhibited selective cytotoxicity on cancer cells, inhibited the Epidermal Growth Factor Receptor (EGFR), increased the intracellular Reactive Oxygen Species (ROS) levels and altered the mitochondrial membrane potential ($\Delta\psi_m$) leading to apoptosis, cell cycle arrest and cancer cell deaths.

Upon treatment of $\text{Pd}(\text{OAc})_2$ (7.5 mol%) and AgOTf (10 mol%) with a mixture of 2-azidobenzaldehyde **1aa**, *tert*-butyl isocyanide **2aa**, tosyl hydrazide **3aa**, phenylacetylene **4aa** and K_3PO_4 in toluene, a four-component adduct, pyrazolo[1,5-c]quinazoline **5aa**, was formed (Scheme 1). The structure of **5** was established by X-ray crystallography¹⁸ and involved the formation of five new chemical bonds in a single operation. Addition of 4 Å molecular sieves was essential to suppress a major side product, urea **7aa** (Scheme 1).¹⁹ Both silver and copper salts worked with equal efficiency in this transformation. Other Pd-sources, bases, and solvents were also screened (for details see section S2 of the Supporting Information), but these turned out to be inferior to the optimal condition. The 4-CR worked well at room temperature, and any further increase in the temperature to 60 °C led to the formation of **9aa**¹⁸ as the major product.



Scheme 1. Reaction condition for four-component reaction.

With an assortment of precursors at hand, a broad diversity of pyrazolo[1,5-c]quinazolines **5** could be constructed from alkynes (Scheme 2, refer Supporting Information for details). The scope of 4-CR was further extended for electron-deficient alkenes, such as acrylates and acrylonitrile, to generate tetrahydropyrazolo[1,5-c]quinazolines **26**¹⁸ of four-point diversity exhibiting excellent atom economy. The investigation underscores high tolerance of the 4-CR reaction to steric and electronic effect. In all cases, the reaction proceeds with high regiochemical fidelity. Interestingly, the formation of a single diastereomer was observed in 4-CR with alkenes.



Scheme 2. Substrate Scope of 4-CR.

The successful isolation of reaction intermediates, carbodiimide **6aa**, and azomethine imine **8aa**¹⁸ (Fig. 2), provided meaningful insights into the mechanism of the 4-CR. **6aa** was readily generated from 2-azidobenzaldehyde **1aa** and *tert*-butyl isocyanide **2aa** was converted to **8aa** upon reacting with the tosyl hydrazide **3aa** (refer Section S5.2 of Supporting Information for details). Interestingly, both steps required Pd(OAc)₂ for catalysis. Conversion of **8aa** to pyrazolo[1,5-*c*]quinazoline **5aa** was catalyzed by silver. Although, these results lend strong support in favor of path A (Fig. 2, *via* **6aa**); an alternate mechanism via **10aa** can also be proposed (Path B). To probe whether the formation of **8aa** could proceed through both path A and path B, or whether one of these pathways was dominating, kinetic studies of 4CR were carried out by monitoring the reaction progress with ¹H NMR spectroscopy (section S5.3). The study unequivocally ruled out path B for the formation of **8aa**. Moreover, the sluggish rate of reaction of the competing concurrent catalytic processes, such as path B, ensured the time-resolution of the relay catalytic process. The regiochemical outcome of 4-CR and H/D scrambling experiment (Section S5.4) revealed that a possible route for the formation of **5aa** is base-mediated direct alkylation of azomethine imine **8aa**. Further, no deuterium incorporation in **5aa** was observed, when the deuterated substrate (ethynyl-*d*)-benzene was reacted with **8aa** (Section S5.5). This observation supports the formation of acetylide during the reaction. Based on experimental studies and literature precedence,²⁰ it is evident that the 4-CR is mediated by three independent catalytic cycles of Pd- and Ag-metals (refer section S5.6 for details).

To explore if the diversity-rich compound collection generated by the bimetallic orthogonal relay catalysis translates into the biological activity, pyrazolo[1,5-*c*]quinazolines **5** and **26** were screened in the MTT based cell viability assay (section S6.2) on cancer cell lines of the lung (A549), colon (HCT-116) and human glioblastoma (U-87 MG) (Table S7). Of these, **5dd**, **5fb**, **26ea** and **26ga** exhibited an excellent cytotoxic effect in all three cancer cells lines. Pleasingly, these compounds also presented negligible toxicity to Human Peripheral Blood Mononuclear Cells (HPBMC) implicating a pattern of selectivity to cancer cells (Section S6.3). Owing to their structural resemblance to the quinazoline scaffold of gefitinib and erlotinib, the investigational compounds **5dd**, **5fb**, **26ea** and

26ga were subsequently scrutinized for inhibition of ATP dependent phosphorylation of EGFR²¹ (Table S8). To our delight, **5fb** was found to be the most potent even with respect to the standard drug, erlotinib, while **5dd** and **26ga** showed comparable activity in the nanomolar range. This observation was further supported by molecular docking studies, which revealed that **26ea** and **26ga** bind to the ATP binding site of EGFR, and exhibit hydrogen bonding interactions with MET769, carboxylate group of **5fb**, and carboxylate group of THR830 and THR766 (Fig. 3 and Section S7).

A further biological investigation revealed that the investigational compounds **5dd**, **5fb**, **26ea** and **26ga** increased the ROS level (section S6.5) and altered the mitochondrial membrane potential ($\Delta\psi_m$) (section S6.6) of pretreated lung cancer cell lines A549. Both these biochemical events play a key role in inducing the mitochondrial apoptosis and lead to lung cancer cell deaths through the ROS-induced mitochondrial-mediated pathway that involves the release of the cytochrome c from the mitochondria into the cytosol. Anticancer drugs are known to delay the progression of cell cycle and inhibit the cell proliferation.²² Analysis of the cell cycle of control and A549 cell lines treated with **5fb** and **26ga** by flow cytometry showed a substantial rise in the G1 phase of cells and the overall drop in the percentage of cycling cells in S phase and G2-M phase (Fig. 4). The G1 phase arrest by investigational compounds may be attributed to the fact that EGFR is a mitogen that helps in cell cycle progression from G1 to G2/M. The CDK4/6 gets inhibited and causes the cell cycle arrest at the G1 phase.²³

Conclusions

In summary, we have developed a novel four-component reaction of 2-azidobenzaldehydes, isocyanides, sulfonyl hydrazides and alkynes/alkenes promoted by orthogonal relay catalysis of Pd(II)/Ag(I). The 4-CR produced a diverse and complex heterocycle, pyrazolo[1,5-*c*]quinazolines with the formation of five new chemical bonds in a single operation. The 4-CR exhibited a broad substrate scope with excellent

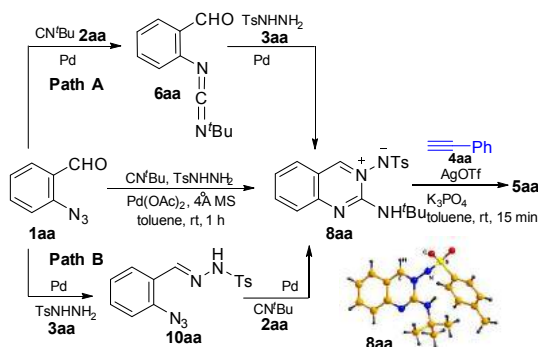


Fig. 2: Control experiments for scrutinizing plausible intermediates.

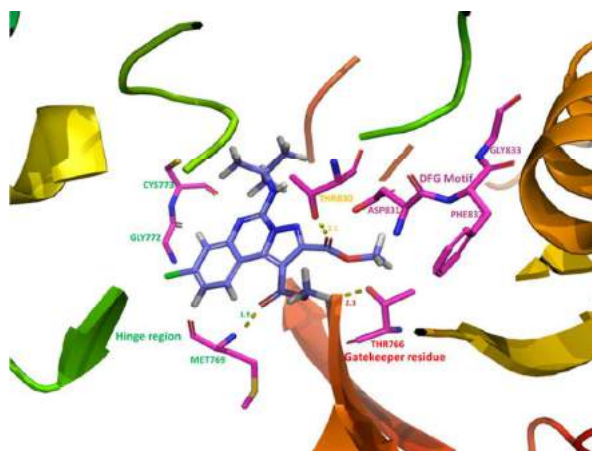


Fig. 3: Binding pattern representation of **5fb** (blue color).

COMMUNICATION

Journal Name

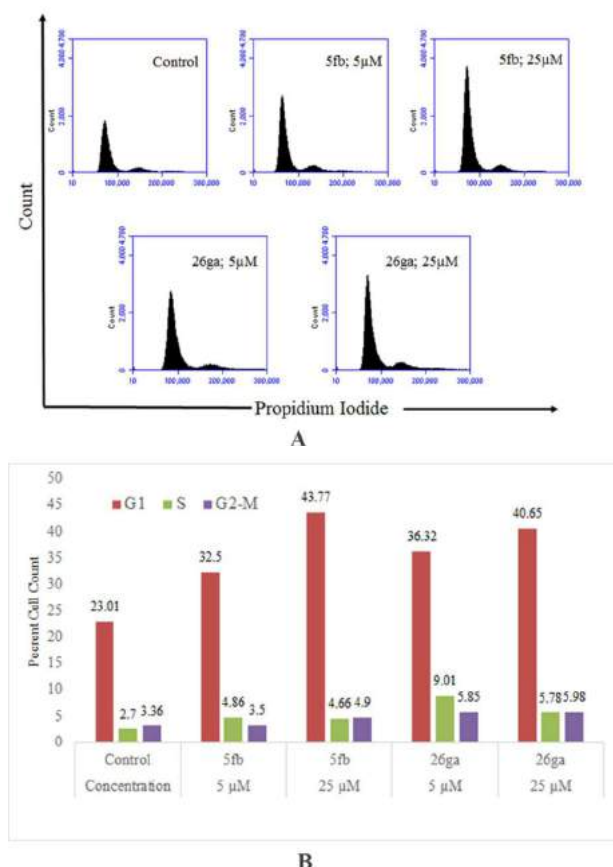


Fig 4. (A) Cell cycle analysis using flow cytometry of A549 cancer cell line treated with **5fb** and **26ga**. (B) The bar graph represents the percent cell count (DNA) at various stages of cell cycle.

regio- and stereocontrol. A focused compound collection of pyrazolo[1,5-*c*]quinazolines exhibited potent and selective cytotoxicity on cancer cell lines. Of these, **5fb** was found two-times potent inhibitor of EGFR than an existing drug, erlotinib. Pyrazolo[1,5-*c*]quinazolines led to the mitochondrial apoptosis through the ROS-induced mitochondrial-mediated pathway that involves the release of the cytochrome *c* from the mitochondria into the cytosol leading to the cytotoxic activity on lung cancer cells (A549) and the cell cycle arrest in G1 phase. The work described herein would pave way for the development of MCR driven design and assembly of bioactive heterocycles.

Conflicts of interest

There are no conflicts to declare.

Notes and references

- L. F. Tietze, G. Brasche and K. Gericke Domino Reactions in Organic Synthesis; Wiley-VCH: Weinheim, Germany, 2006.
- (a) D.-S. Kim, W.-J. Park and C.-H. Jun, *Chem. Rev.* 2017, **117**, 8977-9015; (b) S. M. Inamdar, V. S. Shinde and N. T. Patil, *Org. Biomol. Chem.*, 2015, **13**, 8116-8162.

- (a) Y.-B. Huang, J. Liang, X.-S. Wang and R. Cao, *Chem. Soc. Rev.*, 2017, **46**, 126-157; (b) A. E. Allen and D. W. C. MacMillan, *Chem. Sci.*, 2012, **3**, 633-658.
- (a) N. T. Patil, V. S. Shinde and B. Sridhar, *Angew. Chem.* 2013, **52**, 2251-2255; (b) S.-S. Zhang, J. Xia, J.-Q. Wu, X.-G. Liu, C.-J. Zhou, E. Lin, Q. Li, S.-L. Huang and H. Wang, *Org. Lett.* 2017, **19**, 5868-5871; (c) S.-Y. Chen, Q. Li, X.-G. Liu, J.-Q. Wu, S.-S. Zhang and H. Wang, *ChemSusChem*, 2017, **10**, 2360-2364; (d) S.-S. Zhang, J.-Q. Wu, X. Liu and H. Wang, *ACS Catal.* 2015, **5**, 210-214.
- (a) Z.-P. Yang, W. Zhang and S.-L. You, *J. Org. Chem.* 2014, **79**, 7785-7798; (b) X. Zeng, *Chem. Rev.* 2013, **113**, 6864-6900.
- (a) T. L. Lohr and T. J. Marks, *Nat. Chem.* 2015, **7**, 477-482; (b) N. T. Patil, V. S. Shinde and B. Gajula, *Org. Biomol. Chem.*, 2012, **10**, 211-224.
- S. Chiba, *Chem. Lett.*, 2012, **41**, 1554-1559 and references therein.
- (a) C. K. Prier, D. A. Rankic and D. W. MacMillan, *Chem. Rev.*, 2013, **113**, 5322-5363; (b) M. S. Oderinde, A. Varela-Alvarez, B. Aquila, D. W. Robbins and J. W. Johannes, *J. Org. Chem.*, 2015, **80**, 7642-7651 and references therein.
- L. Zhang, Z. Qureshi, L. Sonaglia and M. Lautens, *Angew. Chem.* 2014, **126**, 14070-14073.
- J. Panteleev, L. Zhang, and M. Lautens, *Angew. Chem.* 2011, **123**, 9255-9258.
- Q. Gao, P. Zhou, F. Liu, W.-J. Hao, C. Yao, B. Jiang and S.-J. Tu, *Chem. Commun.*, 2015, **51**, 9519-9522.
- Z.-S. Chen, X.-Y. Huang, J.-M. Gao, and K. Ji, *Org. Lett.* 2016, **18**, 5876-5879.
- S. Dhiman, U. K. Mishra, and S. S. V. Ramasastry, *Angew. Chem. Int. Ed.* 2016, **55**, 7737-7741.
- W.-W. Ji, E. Lin, Q. Li and H. Wang, *Chem. Commun.*, 2017, **53**, 5665-5668.
- Z.-F. Zhang, D.-X. Zhu, W.-W. Chen, B. Xu and M.-H. Xu, *Org. Lett.* 2017, **19**, 2726-2729.
- A. Galván, F. J. Fañanás and F. Rodríguez, *Eur. J. Inorg. Chem.*, 2016, 1306-1313.
- For various pharmacological activity reported for pyrazolo[1,5-*c*]quinazolines refer Section S9.1
- Characterized by X-ray crystallographic analysis with CCDC numbers 1566282 for **5ad**, 1566285 for **7aa**, 1566284 for **8aa**, 1566283 for **26be** and 1566113 for **9aa**.
- The hydrazone **18** was found extremely prone towards hydration to produce a major side product urea **7aa**. The use of molecular sieves, however could elegantly assist in avoiding this undesired event.
- P. Huang, Q. Yang, Z. Chen, Q. Ding, J. Xu and Y. Peng, *J. Org. Chem.*, 2012, **77**, 8092-8098.
- (a) S. V. Sharma, D. W. Bell, J. Settleman and D. A. Haber, *Nat. Rev. Cancer*, 2007, **7**, 169-181; (b) C. R. Chong and P. A. Jänne, *Nat. Med.*, 2013, **19**, 1389-1400.
- (a) J. D. Ly, D. Grubb and A. Lawen, *Apoptosis*, 2003, **8**, 115-128; (b) E. Gottlieb, M. G. Vander Heiden and C. B. Thompson, *Mol. Cell. Biol.*, 2000, **20**, 5680-5689.
- (a) G. Joshi, H. Nayyar, S. Kalra, P. Sharma, A. Munshi, S. Singh and R. Kumar, *Chem. Biol. Drug Des.*, 2017, **90**, 995-1006; (b) M. Chauhan, G. Joshi, H. Kler, A. Kashyap, S. M. Amrutkar, P. Sharma, K. D. Bhilare, U. C. Banerjee, S. Singh and R. Kumar, *RSC Adv.*, 2016, **6**, 77717-77734.

Relay Tricyclic Pd(II)/Ag(I) Catalysis: Design of a Four-Component Reaction Driven by Nitrene-Transfer on Isocyanide Yields Inhibitors of EGFR

